MRI of the Acute Female Pelvis

11

Joseph W. Owen and Christine O. Menias

Abstract

Magnetic resonance (MR) imaging can be used as a primary or secondary modality in the evaluation of acute pelvic pain in women. MR avoids the ionizing radiation exposure of computed tomography (CT) and provides a larger field of view with greater detail than ultrasound. This chapter first addresses practical considerations including scanner strength, intravenous gadolinium contrast use, and essential MR sequences. Then pelvic inflammatory disease, ectopic pregnancy, and ovarian torsion are reviewed with an emphasis on the MR imaging findings. At the end of this chapter, the reader should be able to structure an MR protocol, implement it in an emergency department setting, and recognize the common causes of acute pelvic pain on MR.

J. W. Owen, M.D.
Department of Radiology, University of Kentucky, Lexington, KY, USA

C. O. Menias, M.D. (✉)
Department of Radiology, Mayo Clinic, Phoenix, AZ, USA
e-mail: Menias.Christine@mayo.edu

11.1 Introduction

Magnetic resonance (MR) imaging has sufficient spatial resolution and soft-tissue contrast to accurately diagnose most disease processes presenting as acute pelvic pain. Ultrasound (US) is the preferred initial modality used for the evaluation of pelvic pain due to its low cost and absence of ionizing radiation, but US has limitations, and additional cross-sectional imaging is often needed in women presenting with acute pelvic pain. In a study of pregnant women presenting with acute pain, 30% of CT scans performed after a normal US showed acute pathology [1]. CT is widely available, but growing societal concern over ionizing radiation has led to increased use of MR in place of CT, particularly in children, women of reproductive age, and pregnant women.

MR imaging is now available 24/7 in many hospitals with busy emergencies departments, driven in part by neuroimaging, and can be an effective tool for body imagers. Radiologists can facilitate adoption of MR in the emergency department by streamlining patient screening/scheduling, developing efficient MR protocols, and ensuring that the radiologists responsible for covering the emergency department are familiar with acute MR findings. Most gynecologic emergencies are traditionally characterized with ultrasound, and many radiologists in the past have not been exposed to MR imaging of acute pelvic pain

M. Patlas et al. (eds.), *MDCT and MR Imaging of Acute Abdomen*,
https://doi.org/10.1007/978-3-319-70778-5_11

during training. The classic US findings are often translatable to MR, however, and much of the literature promoting the use of MR for acute body imaging is descriptive [2–7]. Peer-reviewed scientific publications are more limited, but have revealed instances when MR can be prognostic or affect patient management.

This chapter will address the practical aspects of implementing MR imaging for acute pelvic pain in the ER, and then will review the MR features of the most common gynecologic emergencies.

11.2 MR Protocol

11.2.1 Magnetic Strength

Both 1.5 Tesla and 3 Tesla MR scanners can be used to image the female pelvis, with minor trade-offs in image quality, acquisition time, and availability. A comparison of 1.5 T and 3 T MR imaging of the female pelvis showed similar overall image quality [8], with increased motion artifacts on 1.5 T images, and increased inhomogeneity on 3 T images. Qualitative evaluation of the cervix, vagina, and ovaries was better at 3 T than at 1.5 T. The improved spatial resolution of 3 T may be necessary for staging gynecological malignancy [9], but the minor differences in image quality are unlikely to impact the diagnosis of acute pathology. An optimized 3 T protocol just can permit fast acquisitions (less than 10 min) which are motion insensitive and high resolution [10], but 1.5 T scanners are more widely available and have less competition with acute neuroimaging examinations for MR scanner time. 3 T scanners are preferable for pelvic imaging, but quality diagnostic imaging can be achieved with either field strength with optimized protocols.

In pregnant women there are theoretical risks of fetal heating and fetal hearing damage from MR scanning. No adverse effects have been reported in any trimester at 1.5 T or 3 T, to our knowledge; however, the American College of Radiology guidelines on MR safety recommend screening of reproductive age women for pregnancy before MR, but there is no contraindication to MR imaging at 3 T or 1.5 T during the first trimester, or at any other point during pregnancy. Some institutions may choose to obtain written informed consent prior to MR scanning in known pregnant patients, but this is not a universal practice [11]. The radiologist ideally should monitor these examinations and use only the necessary sequences in pregnant patients.

11.2.2 Gadolinium Contrast

Gadolinium-based intravenous contrast agents are routinely used when imaging the female pelvis, if not contraindicated due to allergy, impaired renal function, or pregnancy. Intravenous contrast is not as essential for MR imaging of the pelvis as it is for CT, since enhancement patterns are often less important than anatomic and morphologic changes evident on noncontrast imaging.

Gadolinium-based intravenous contrast agents have a good safety profile in properly selected nonpregnant patients. Mild nonallergic adverse reactions are much more common than allergic reactions, and fatal reactions are rarely reported [12]. There is little evidence to support premedication with corticosteroids and diphenhydramine, but premedication is still recommended in the rare person with a prior allergic reaction to gadolinium-based intravenous contrast agents. Where the reaction was mild/relatively mild, and the repeat use of IV gadolinium contrast material is otherwise indicated. Premedication prior to intravenous gadolinium is not recommended in those with documented allergy to iodinated contrast agents or "shellfish."

Patients with impaired renal function are at risk for the development of systemic nephrogenic fibrosis, and gadolinium-based intravenous contrast agents should be restricted in patients with a glomerular filtration rate of 15–30 mL/min/1.73 m^2, and should be avoided in patients with a glomerular filtration rate of <15 mL/min/1.73 m^2. If gadolinium is to be administered to a patient with impaired renal function, lower-risk gadolinium-based agents including gadobutrol (Gadovist®, Gadavist®), gadoterate meglumine (Dotarem®, Magnescope®), or

gadoteridol (Prohance®) should be used when available [13].

GBCAs are not routinely administered to pregnant patients or to patients with suspected pregnancy. No adverse outcome to the mother or fetus in humans has been reported after GBCA administration to our knowledge, but no large trial has assessed its safety. GBCAs have been shown to cross the placenta and to accumulate in amniotic fluid. This creates the potential for prolonged gadolinium exposure to the fetus and mother, and a theoretical risk of connective tissue disease. The limited potential benefit of GBCAs administration in pregnant women outweighs potential risks in most patients [12]. GBCAs administration can be considered selectively in patients with nonviable pregnancy, known extrauterine gestation, or pregnancy of unknown location.

11.2.3 Essential MR Sequences

T2-weighted sequences are the foundation of pelvic MR imaging, with T1-weighted in- and opposed-phase, post-contrast T1-weighted, diffusion-weighted, and balance steady-state free-precession sequences adding complementary information. A basic examination should start with partial Fourier single-shot turbo spin-echo sequences (HASTE, SS-TSE, SS-FSE) in the coronal, axial, and sagittal planes, a T2-weighted fast spin-echo sequence with fat suppression in the axial plane, and T1-weighted in- and opposed-phase sequences in the axial plane.

The single-shot turbo spin-echo sequences are preferably breath-hold acquisitions, but can be performed with free breathing. They are relatively motion insensitive and often provide sufficient anatomic detail for initial differential diagnosis. The axial T2-weighted turbo spin-echo (TSE) sequence with fat suppression (FS) complements the single-shot technique by increasing the conspicuity of cysts, free fluid, edema, and inflammation. The axial gradient-recalled echo (GRE) T1-weighted in- and opposed-phase sequence helps with the identification of blood products, fat-containing masses - particularly dermoid cysts - and can accentuate pathologic gas.

If gadolinium-based intravenous contrast agents are used, an axial pre-contrast T1-weighted gradient-recalled echo (GRE) sequence with fat suppression (VIBE, LAVA, or THRIVE) precedes a post-contrast sequence, with the same imaging parameters. Sagittal and coronal post-contrast images are often helpful and may be added if the examination is not time constrained. Post-contrast imaging permits characterization of focal abnormalities, hyperemic or inflamed tissue, demonstrates vessel patency, and may show nonenhancement of a torsed ovary. If intravenous gadolinium is not administered, a steady-state free-precession sequence (TrueFISP, Balanced FFE, or FIESTA) can be added to characterize the patency of the pelvic vasculature.

Diffusion-weighted imaging (DWI) should be considered in all patients undergoing pelvic MR and is increasingly seen as an essential sequence with a growing body of evidence supporting its use. Abscesses, masses, lymphadenopathy, and inflammation are made more conspicuous on DWI. Small studies have shown improved characterization of pelvic inflammatory disease [14], ovarian vein thrombophlebitis, and hemorrhagic infarction of a torsed ovary [15, 16] when DWI is employed. If high-quality DWI is routinely obtained, the low *B*-value sequence may function in place of the axial T2 fast spin-echo fat-suppressed sequence, to save time, as low *B*-value DWI is essentially a heavily T2-weighted fat-suppressed sequence.

11.3 Pelvic Inflammatory Disease

11.3.1 Background

Pelvic inflammatory disease (PID) is classified into three distinct subtypes: acute, subacute, and chronic. Acute PID manifests in less than 30 days and often presents with acute pelvic pain, vaginal discharge, abnormal vaginal bleeding, dyspareunia, and dysuria. It is caused by ascending infection of sexually transmitted diseases, bacterial vaginosis, or gastrointestinal or respiratory flora colonized in the vagina [17, 18]. The ascending infection progresses along a continuum from cervicitis to endometritis, salpingitis,

tubo-ovarian abscess, and peritonitis [19, 20]. Acute PID occasionally presents as right upper quadrant abdominal pain due to peritoneal spread of infection resulting in perihepatitis, also known as Fitz-Hugh-Curtis syndrome [21, 22], with recent reports showing perihepatitis in upwards of 50% of patients with PID [23]. Subclinical PID is a low-grade infection, typically caused by chlamydia or gonorrhea, and often manifests as tubal occlusion-related infertility. It may be incidentally detected as an asymptomatic hydrosalpinx on MR, but rarely presents as acute pain. Chronic PID is relatively rare and is associated with *Mycobacterium tuberculosis* and actinomycosis infection. The sensitivity of MR for revealing subtle inflammation makes it a useful tool to reinforce the clinical and laboratory signs of pelvic inflammatory disease and can impact treatment planning [18].

11.3.2 Epidemiology

The U.S. Centers for Disease Control estimate the lifetime prevalence of pelvic inflammatory disease (PID) to be 4.4%, with approximately 2.5 million American women age 14–44 experiencing at least 1 episode [24]. The incidence of PID has been decreasing in North America and Europe over the past 30 years [25, 26], possibly due to improved screening for chlamydia and gonorrhea in asymptomatic sexually active women [27].

Risk factors for pelvic inflammatory disease include prior incidence of sexually transmitted infection, early first sexual encounter, increasing number of partners, and homosexual or bisexual orientation. No difference in prevalence was found with age, race, ethnicity, or socio-economic status [24].

11.3.3 MR Findings

Cervicitis commonly presents as mucopurulent endocervicitis, with approximately 40% of cases due to gonorrhea, chlamydia, or trichinosis, and 60% of cases due to unknown pathogens [28, 29]. Visual inspection demonstrates mucopurulent discharge from the cervix, with easily inducible bleeding, and >10 white blood cells on gram stain. Isolated cervical infection is often asymptomatic and is diagnosed on routine physical examination or on sexually transmitted disease screening.

MR imaging of isolated cervicitis may be normal, but a spectrum of nonspecific findings may increase the suspicion for infection. The normal cervix has three defined layers on T2-weighted sequences, with a T2 hyperintense endocervical inner layer, a T2 hypointense fibrous stroma, and a T2 intermediate signal cervical myometrium [30–32] (Fig. 11.1). When infection is present, the cervix may enlarge, and the endocervical tissue may thicken. The thickened endocervix can show hyperenhancement on post-contrast images. Parametrial fat stranding related to inflammation may cause the outer margin of the cervix to become indistinct [33, 34] on T2- and T1-weighted MR images (Fig. 11.2). In subacute and chronic infection, focal T2 hyperintense, and T1 intermediate to hyperintense cysts can develop in the endocervix [31]. The endocervical cysts can be indistinguishable from nabothian cysts, and it is believed that nabothian cysts may be the result of chronic or healed inflammation related to cervicitis [35, 36].

Endometritis can result from ascending infection from the cervix along the PID continuum [20], but is more commonly seen in the postpartum period after prolonged rupture of membranes, intra-partum fever, chorioamnionitic, or cesarean section [37, 38]. As with other forms of PID, endometritis presents along a spectrum of acuity, with chronic colonization of the endometrium often manifesting as infertility due to poor implantation [39], and acute infections, often related to gonorrhea and chlamydia, presenting with pelvic pain. PID related acute endometritis may present as nonspecific pelvic pain, with abnormal vaginal discharge, but no fever or leukocytosis. Bimanual examination may reveal cervical motion tenderness or uterine tenderness, but routine abdominal palpation may be normal

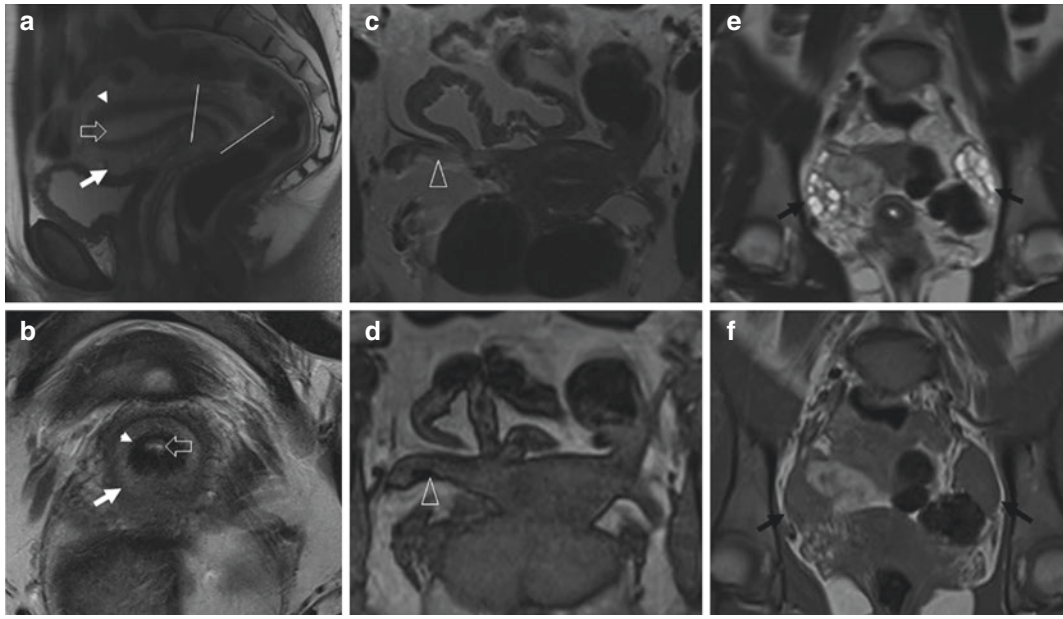

Fig. 11.1 Normal pelvic anatomy—(**a**) Sagittal and axial (**b**) T2-weighted MR images demonstrating the three layers of the uterus and cervix. Hyperintense endometrium/endocervix (open arrow), hypointense junctional zone/cervical fibrous stroma (arrowhead), and intermediate intensity uterine/cervical myometrium (white arrow). The cervix is demarcated by white lines. (**c**) Axial T2-weighted and (**d**) opposed-phase T1-weighted MR images demonstrating a normal fallopian tube (open arrowhead). (**e**) Coronal T2-weighted and (**f**) T1-weighted MR images demonstrating normal ovaries with physiologic follicles

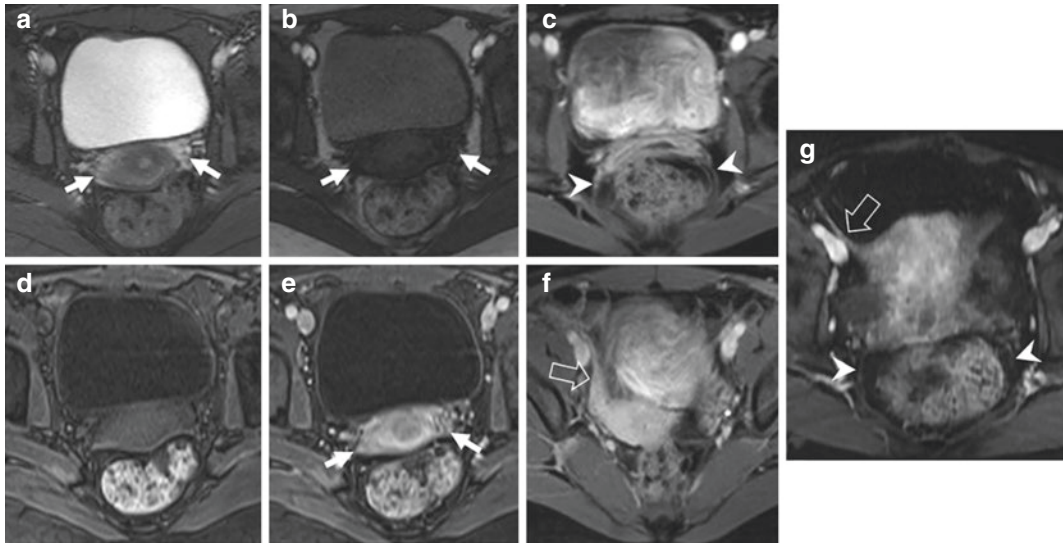

Fig. 11.2 Cervicitis—(**a**) T2-weighted and (**b**) opposed-phase T1-weighted MR images showing indistinct margins of the cervix due to parametrial stranding and edema in a patient with cervicitis. (**c**) Pre-contrast T1-weighted and (**d**) post-contrast T1-weighted MR images demonstrating enhancement of the parametrial fat. (**e** and **f**) Post-contrast T1-weighted MR images demonstrating uterosacral ligament thickening (open arrow) and round ligament thickening (arrowheads). (**g**) Post-contrast T1-weighted MR images demonstrating normal uterosacral ligaments (arrowheads), and a normal round ligament (open arrow) for comparison

in the absence of salpingitis, tubo-ovarian abscess, or peritonitis [20].

The normal uterus has three distinct layers on MR: the well-defined T2 hyperintense endometrium, the T2 hypointense poorly marginated junctional zone, and the T2 intermediate intensity myometrium (Fig. 11.1). MR may be normal in isolated endometritis, but when abnormal, endometritis manifests as thickened heterogeneous endometrium, with hyperenhancement. T1 intermediate fluid may fill the endometrial canal. Intra-cavitary gas can be seen as multifocal signal voids on the T1-weighted in-phase MR images, and is more common in post-partum endometritis. As with cervicitis, parametrial fat stranding may be present, is most evident on T2-weighted fat-suppressed MR imaging, and may result in indistinct outer margins of the myometrium. Round ligament and uterosacral ligament thickening are sensitive signs for PID [33, 40–43] and should trigger close inspection for more specific signs of infection (Fig. 11.2).

Salpingitis results in degeneration of the tubal epithelium, deciliation, decreased mucosal fold density, peritubal adhesions, partial or complete tubal occlusion, and hydrosalpinx [44]. Salpingitis may present with acute symptoms or can be clinically asymptomatic, but acute and silent cases have similar histology, and both result in decreased fertility and increased risk of ectopic pregnancy. In addition to the signs and symptoms of cervicitis and endometritis, salpingitis may manifest as pelvic tenderness to palpation and adnexal tenderness on bimanual examination [20].

On MR, the normal fallopian tubes are barely perceptible, 1–4 mm thick, serpentine, T2 intermediate intensity structures extending from the uterine cornua to the ovary [45] (Fig. 11.1). MR of salpingitis reveals a mildly dilated, tortuous fallopian tube, with a thin or slightly thickened wall. There may be perceptible enhancement of the wall, and peritubal fat stranding. The fallopian tube will have T1 hypointense, T2 hyperintense, and simple fluid without diffusion restriction. Acute or subacute salpingitis may not be distinguishable from chronic hydrosalpinx related to prior salpingitis. Incomplete longitudinal folds from mucosal plicae may be seen, but with more severe dilation, the plicae become effaced [14, 45]. Mild thickening of the round ligament and uterosacral ligaments, in this setting, are associated with acute infection. Isolated tubular torsion is a rare, but reported cause of acute pelvic pain, which may be indistinguishable from salpingitis, hematosalpinx, or hydrosalpinx [14], but which is often associated with "beaking" or a closed-loop appearance of the torsed fallopian tube [46, 47] (Fig. 11.3).

Pyosalpinx and tubo-ovarian abscess constitute severe forms of PID and often require hospitalization for inpatient therapy or intervention. Up to one-third of patients hospitalized with severe PID will have a tubo-ovarian abscess [48]. Women hospitalized for PID should undergo cross-sectional imaging [20] to assess for abscesses greater than 5 cm, as these may require drainage. Most patients present with infectious symptoms including fever, leukocytosis, and acute pelvic pain; however, a subset of patients with tubo-ovarian abscess have low-grade symptoms including chronic fever of unknown origin or have a remote history of sexually transmitted infection treated with antibiotics [49]. Physical examination reveals tenderness to palpation, and tender adnexal fullness or masses on bimanual examination. While ultrasound remains the first-line imaging modality, MR or IV contrast-enhanced CT are often required to fully characterize pyosalpinx and tubo-ovarian abscess.

MR of pyosalpinx shows a dilated tortuous tubular structure, with a thick enhancing wall, surrounding fat stranding, and thickening of the adjacent fascial planes [14, 33, 45, 50, 51]. The dilated fallopian tube is filled with T2 hyperintense or heterogeneous fluid which has variable T1 intensity related to the presence of pus, blood, or protein. The fluid is hyperintense on diffusion-weighted imaging and hypointense on ADC maps [14]. The morphology of the tube is often described as sausage-like, c-shaped, or s-shaped. The thickened wall is T1 hypointense, T2 intermediate to hyperintense, and markedly enhances. Pyosalpinx is not always distinguishable from

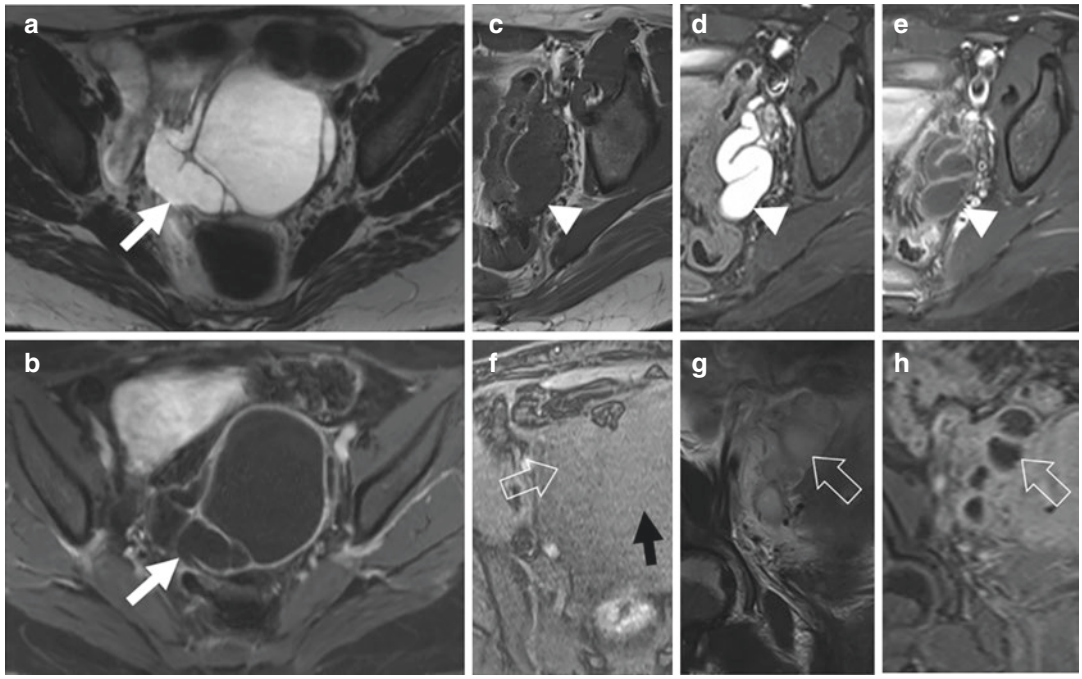

Fig. 11.3 Hydrosalpinx, salpingitis, and pyosalpinx—(**a**) T2-weighted and (**b**) post-contrast T1-weighted MR images demonstrating chronic hydrosalpinx with a dilated fallopian tube, a thin enhancing wall and simple fluid (white arrow). (**c**) T1-weighted, (**d**) T2-weighted FS, and (**e**) post-contrast T1-weighted MR images demonstrating salpingitis with an s-shaped, dilated fallopian tube (arrowhead), simple fluid, a mildly thickened enhancing wall, and mild peritubal stranding. (**f**) Opposed-phase T1-weighted, (**g**) T2-weighted, and (**h**) post-contrast T1-weighted MR images demonstrating pyosalpinx (open arrow), with a dilated fallopian tube, T1 and T2 intermediate intensity complex fluid, thick enhancing walls, and marked adnexal inflammation. Note the T1 signal intensity within the tube is similar to myometrium (black arrow)

hydrosalpinx, but tends to have more wall thickening and T2 heterogeneous fluid than expected with the simple fluid of hydrosalpinx, or salpingitis. Pyosalpinx can mimic inflamed or obstructed bowel, and is distinguished by its location in the adnexa, continuity with the uterine cornua, and lack of continuity with bowel. Concomitant bowel inflammation and obstruction can occur, especially if peritonitis or tubo-ovarian abscess is present. At times, the diagnosis of TOA on MR may be challenging in patients with inflammatory bowel disease, as these patients may present with active bowel inflammation which may also involve the adnexa, resulting in inflammation and tubo-ovarian abscesses. Careful review of the bowel and epicenter of the inflammation can be useful to help distinguish between these two diagnoses (Fig. 11.3).

Tubo-ovarian abscesses are complex cystic adnexal masses, which often result in severe surrounding inflammation. Mild forms of ovarian inflammation associated with PID are described as oophoritis and manifest as periovarian stranding and ovarian enlargement. Progression of inflammation beyond oophoritis may lead to tubo-ovarian abscess. Tubo-ovarian abscesses have T2 hyperintense or heterogeneous cystic spaces with variable T1 intensity and may demonstrate a thin inner rim of T1 hyperintensity [52]. Enhancing internal septations often create a multiloculated appearance. The margins of tubo-ovarian abscesses are indistinct on T2- and T1-weighted imaging due to adjacent edema and exudate. Diffusion-weighted images show hyperintense fluid with low signal on ADC [14]. Dense surrounding adhesions result in distortion of the

local anatomy. Adhesions are T2 hypointense and T1 hypointense, with mild enhancement. Free fluid, periovarian stranding, thickening of the pelvic fascial plains, round ligaments and uterosacral ligaments, smooth peritoneal enhancement, adjacent bowel wall thickening, and lymphadenopathy are all common features [23, 42, 49, 52]. Rupture of a tubo-ovarian abscess may lead to severe peritonitis, sepsis, and if treatment is delayed, rarely death (Figs. 11.4 and 11.5).

Distinguishing features of tubo-ovarian abscess from cystic ovarian neoplasm include associated fallopian tube dilation [52], a T2 hyperintense peri-cystic "halo" of edema [49], smooth peritoneal enhancement as opposed to nodular enhancement, and absence of enhancing soft-tissue nodules. Pus can appear "pseudo-solid" with T1 intermediate intensity, variable T2 intensity, and restricted diffusion, but the "pseudo-solid" areas of diffusion restriction in tubo-ovarian abscess should not enhance [14]. Necrotic and/or cystic components of an ovarian neoplasm do not typically restrict diffusion.

Thrombophlebitis of the ovarian vein can be a complication of PID, but is more common in post-partum women or women with recent pelvic surgery, and is rarely life threatening. It is often asymptomatic, detected incidentally, and can be treated with anticoagulation. MR is highly sensitive for the demonstration of ovarian vein thrombophlebitis [53], with improved characterization when MR venography sequences are employed [54]. Partial Fourier single-shot turbo spin-echo images are susceptible to flow artifacts within the veins, but loss of signal void within the vein and venous enlargement should prompt closer inspection. Thrombus is often T2 intermediate to hyperintense and is associated with perivascular stranding. Stranding may be more evident on T2-weighted fat-suppressed images or on low *B*-value diffusion-weighted images. On T1-weighted images, thrombus can appear with T1 hypointensity or hyperintensity within the vessel [55]. Post-contrast images or balanced steady-state free-precession MR images will demonstrate loss of signal with the lumen of the dilated ovarian vein. Thrombus is hyperintense on DWI and hypointense on ADC images [56].

Actinomycosis is a rare form of severe pelvic inflammatory disease which is associated with the protracted presence of intrauterine devices or pessaries. Women with IUDs have reported colonization rates of 1–14% [57, 58]. Actinomycosis infection is often mistaken as malignancy, and the presence of an IUD should raise suspicion for infection when a complex adnexal mass is detected [59, 60].

Pelvic actinomycosis often presents with abdominal pain, vaginal bleeding, fever, anemia, and leukocytosis, although in approximately one-fifth of patients the findings are detected incidentally on imaging [61]. On CT and MR, pelvic actinomycosis presents as an invasive heterogeneous mass [60, 62] which obliterates the tissue planes of the pelvis. It tends to invade the rectum and the bladder [61], sometimes extending through the abdominal and pelvic wall. Compared with malignancy, the soft-tissue components tend to be T2 hypointense [60], and extend in thick linear bands throughout the pelvis without respecting tissue planes [63]. Scatter cystic spaces are common and may represent small abscesses [63]. There is marked enhancement of the soft-tissue components, and on FDG-PET the soft-tissue components may demonstrate FDG avidity [64].

11.3.4 Management

Pelvic inflammatory disease has a broad range of severity, which impacts treatment strategies. Mild to moderate pelvic inflammatory disease can be managed with outpatient therapy, typically a combination of intramuscular cephalosporin and oral doxycycline with or without metronidazole [65]. Lack of symptomatic improvement with 72 h of outpatient therapy may require parenteral therapy, repeat imaging, and hospitalization. Patients who are clinically unstable, have refractory nausea and vomiting or high fever, cannot tolerate oral antibiotics, are pregnant, or have a tubo-ovarian abscess require hospitalization, imaging, and parenteral antibiotics. Typical regimes include oral/IV doxycycline and an IV cephalosporin, or IV clindamycin and gentamycin. Inpatients can be transitioned to oral antibiotics with 24 h of clinical improvement [18, 66].

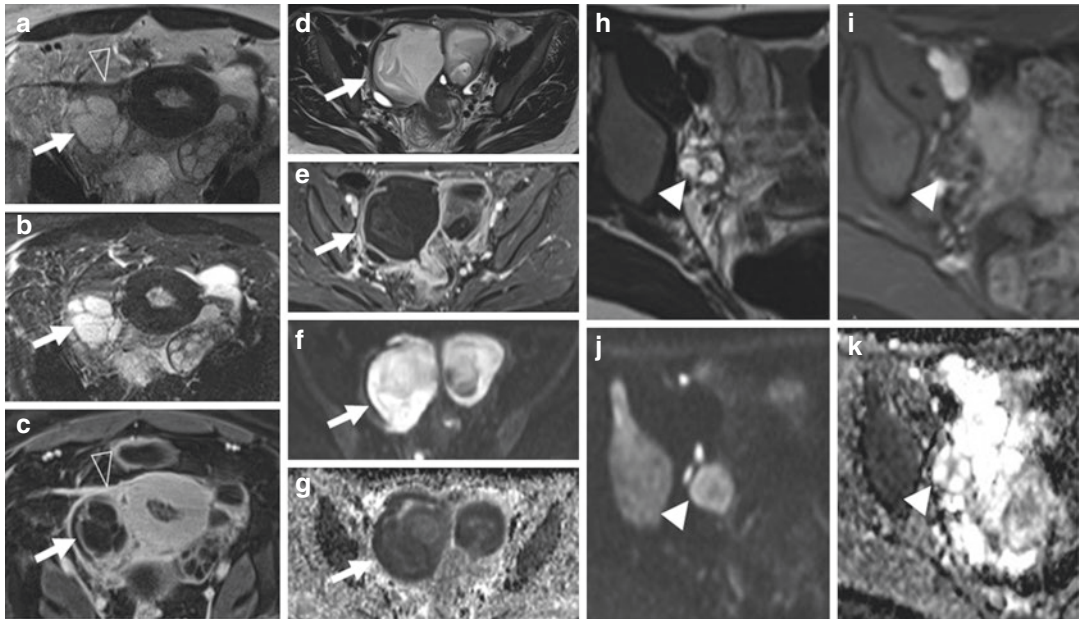

Fig. 11.4 Tubo-ovarian abscesses—(**a**) T2-weighted, (**b**) T2-weighted FS, and (**c**) post-contrast T1-weighted MR images demonstrating a tubo-ovarian abscess with a multiloculated cystic mass (white arrow), with enhancing septations, adnexal stranding, and round ligament thickening (open arrowhead). (**d**) T2-weighted, (**e**) T2-weighted FS, (**f**) DWI, and (**g**) ADC MR images showing a different tubo-ovarian abscess (white arrow) with complex fluid that restricts diffusion. (**h**) T2-weighted, (**i**) post-contrast T1-weighted, (**j**) DWI, and (**k**) ADC MR images showing a normal ovary with physiologic follicles for comparison

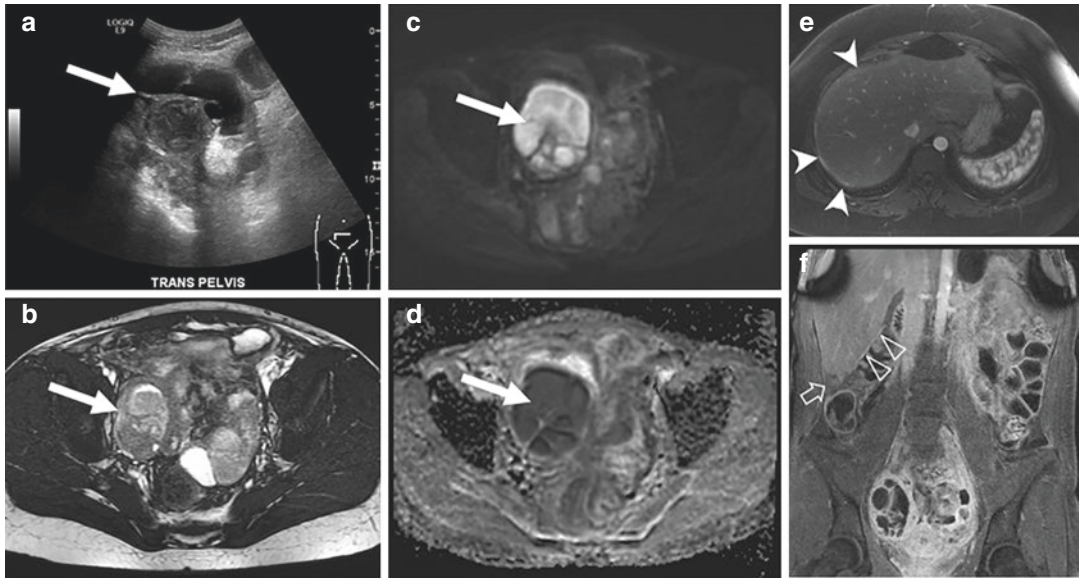

Fig. 11.5 Tubo-ovarian abscess with perihepatitis—(**a**) ultrasound demonstrating a complex adnexal mass (white arrow). (**b**) T2-weighted MR image confirming the complex cystic mass (white arrow) in the right adnexa. (**c**) DWI and (**d**) ADC MR images showing diffusion restriction in the cystic portions of the mass, compatible with abscess. (**e**) T2-weighted FS image showing T2 hyperintensity along the liver capsule (arrowhead) and (**f**) coronal post-contrast T1-weighted MR image showing pericapsular enhancement (open arrowhead) and a small complex fluid collection (open arrow), representing the perihepatitis of Fitz-Hugh-Curtis syndrome

Stable patients with tubo-ovarian abscess may be initially treated with parenteral antibiotics. Patients without resolution of pain and fever in 48–72 h may require repeat imaging and imaged-guided percutaneous drainage. Tubo-ovarian abscesses over 5 cm have a high rate of antibiotic therapy failure and often require percutaneous drainage [67]. Multiple reports advocate primary percutaneous drainage and antibiotics as a safe and effective treatment for tubo-ovarian abscesses larger than 5 cm. Surgical intervention is often unnecessary with the widespread availability of image-guided minimally invasive techniques, but laparoscopic drainage may be necessary if an abscess cannot be safely accessed percutaneously or if interventional radiology services are unavailable [67–70].

Detection of ovarian vein thrombophlebitis warrants treatment with anticoagulation to prevent pulmonary embolism. Patients failing anticoagulation with breakthrough pulmonary embolus may need a suprarenal inferior vena cava filter. The majority of patients will recanalize their ovarian vein with anticoagulation, but may experience long-term sequelae, including recurrent deep venous thrombosis and pelvic venous congestion syndrome from ovarian vein valvular incompetence [71]. Work-up for hypercoagulability disorders should be considered after the diagnosis of ovarian vein thrombophlebitis, in the absence of a predisposing condition such as recent surgery or infection.

If actinomycosis infection is suspected, due a locally invasive inflammatory process and an IUD, aspiration is recommended to confirm the diagnosis. Unfortunately, actinomycosis is a gram-positive anaerobic bacteria, which is difficult to culture, and many patients with surgically confirmed actinomycosis infection are culture negative [72]. Proper anaerobic sampling technique [73] combined with gram stain and hematoxylin and eosin stain can improve sensitivity [74]. Primary resection is difficult and initial treatment with long-term high-dose antibiotics is recommended [75]. Resection may be done secondarily to remove or divert portions of the genital, urinary, or gastrointestinal tract, due to fistula or obstruction.

11.4 Ovarian Torsion

11.4.1 Background

Ovarian torsion occurs due to rotation of the ovary around the vascular pedicle, resulting in ischemia of the ovarian tissue. With progressive rotation of the ovary around the pedicle, there is first compromise of the venous outflow, followed by compromise of the arterial supply. This results in enlargement of the ovary with subsequent ischemia. Ischemia may progress to hemorrhagic infarction and necrosis if not quickly diagnosed and treated. The diagnosis of ovarian torsion is often delayed due to a nonspecific clinical presentation [76], and the potential for intermittent torsion adds to the diagnostic challenge.

Ovarian torsion classically presents with sudden onset, moderate to severe, sharp stabbing, lower quadrant pain, which may radiate to the back, flank, or groin [77]. The pain can be subacute or chronic in a substantial subset of patients [78], particularly those with intermittent or partial torsion. A palpable mass may be evident on physical examination; however, one-third of patients have no mass or tenderness. Presentation after onset of pain is reportedly as short as 4 h in 80% of patients [79], but can be considerably longer with intermittent or partial torsion.

Ovarian torsion has been extensively characterized with ultrasound in the literature, but due to its nonspecific presentation and because of this initial imaging is often performed with CT. Even when ultrasound is performed first, Doppler US demonstrates adnexal blood flow in 20–50% patients with confirmed ovarian torsion [77, 78, 80], likely due to the ovary's dual blood supply. When US or CT demonstrates an adnexal mass in the setting of acute or subacute pelvic pain, or when ultrasound is equivocal, MR may be performed for additional characterization of the abnormal adnexa [81]. MR is highly sensitive and specific for torsion when used as a primary modality, or after indeterminate US or CT [79, 82] (Fig. 11.6).

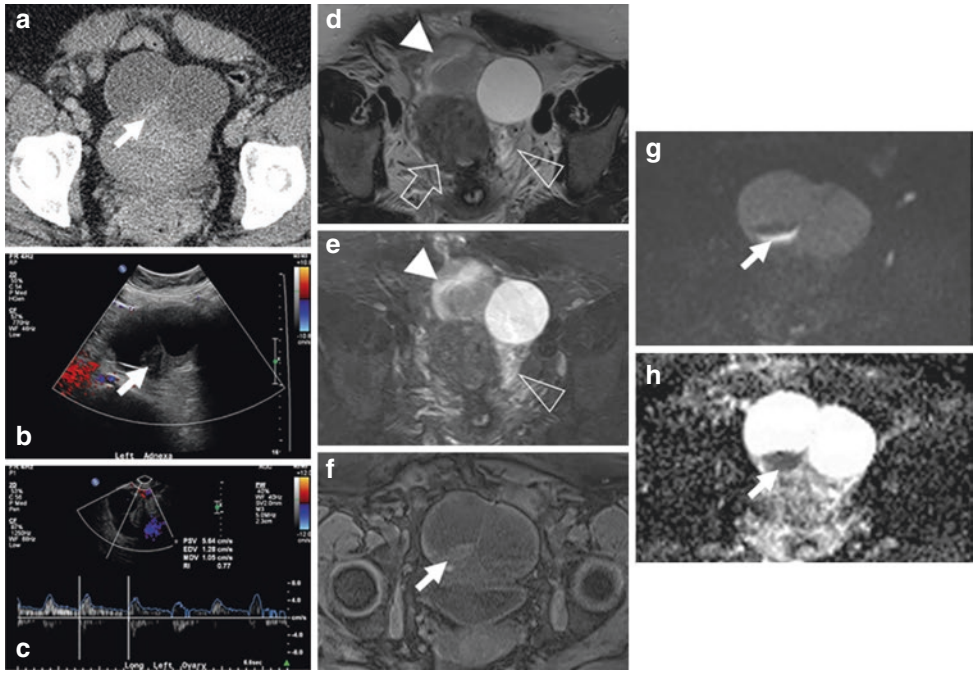

Fig. 11.6 Ovarian torsion—(**a**) CT image showing an enlarged torsed ovary (black arrow) eccentrically positioned anterior to the uterus with 2 cysts. (**b**) Color Doppler and (**c**) spectral wave Doppler US showing an enlarged hypovascular ovary, but detectable arterial flow. (**d**) T2-weighted and (**e**) T2-weighted FS MR images showing the eccentric anteriorly positioned torsed ovary, with a hemorrhagic cyst (white arrowhead), thickened and edematous pedicle (open arrowhead), and deviated uterus (open arrow). (**f**) T1-weighted FS, (**g**) DWI, and (**h**) ADC MR images demonstrating layering hemorrhage and an adjacent rim of diffusion restriction (white arrow) at the interface of the cyst and the ovarian tissue

11.4.2 Epidemiology

Ovarian torsion is an uncommon condition, predominately described with single institutional experience, and few large epidemiologic studies characterize its incidence to our knowledge. Early reports estimate that 2.7% of acute gynecologic emergencies are due to ovarian torsion [76], which is similar to a recent report by Petkovska et al. [83]. One population-based epidemiologic study from South Korea showed an incidence of 5.9/100,000 in women of all ages, and 9.9/100,000 in reproductive age women [84].

Multiple conditions have been implicated as risk factors for ovarian torsion. Ovarian cysts and ovarian neoplasms are well-recognized risk factors for torsion, with 25–80% [77, 78] associated with a cyst (Fig. 11.7). Prior pelvic surgery, specifically prior tubal ligation, is an important risk factor for ovarian torsion, with 40–50% of patients having a history of surgery [77, 80]. Adhesions from tubal ligation, or other procedures, may serve as a pivot point for rotation of the ovary around the vascular pedicle. Prior PID is a risk factor, presumably for a similar reason, with peritubal adhesions a common sequela of salpingitis. Treatment for infertility, specifically hormonal stimulation, is an increasingly important etiology for ovarian torsion, especially when infertility treatment results in pregnancy [85, 86] (Fig. 11.8).

11.4.3 MR Findings

Thickening of the twisted vascular pedicle and fallopian tube is frequently evident on MR in the

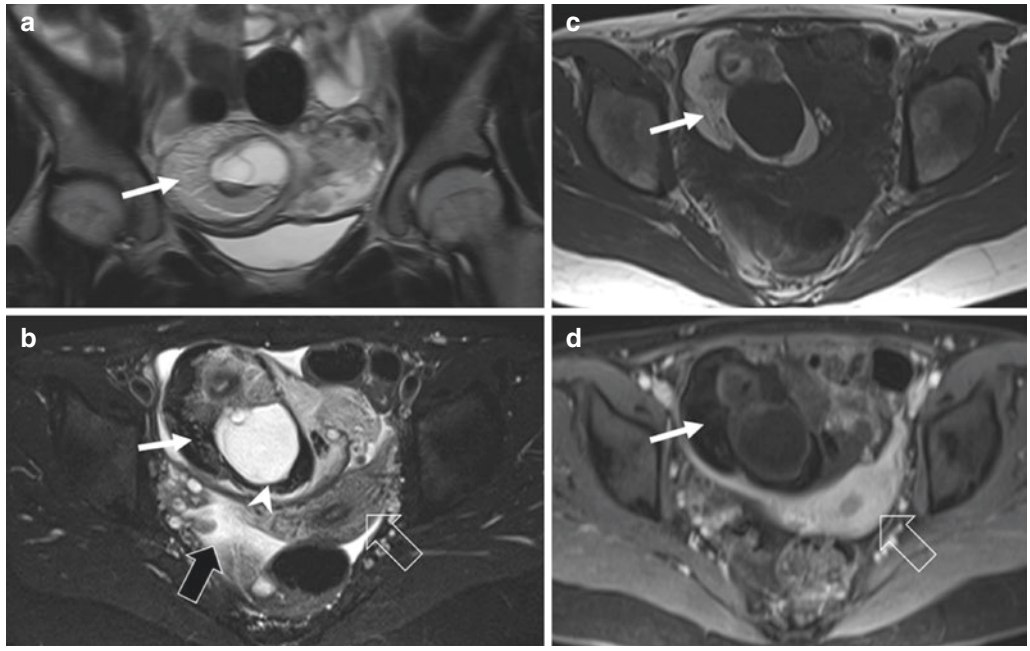

Fig. 11.7 Ovarian torsion with teratoma—(**a**) Coronal T2-weighted and (**b**) axial T2-weighted FS MR images demonstrating a complex cystic right adnexal mass with T2 hyperintense soft-tissue which becomes hypointense with fat suppression, representing a cystic teratoma (white arrow). The same soft tissue shows T1 hyperintensity with fat suppression and no enhancement on (**c**) pre-contrast T1-weighted and (**d**) post-contrast T1-weighted FS MR images. There is associated uterine deviation (open arrow), wall thickening of the cystic lesion (arrowhead), free fluid, edema (black arrow), and anterior positioning of the torsed ovary

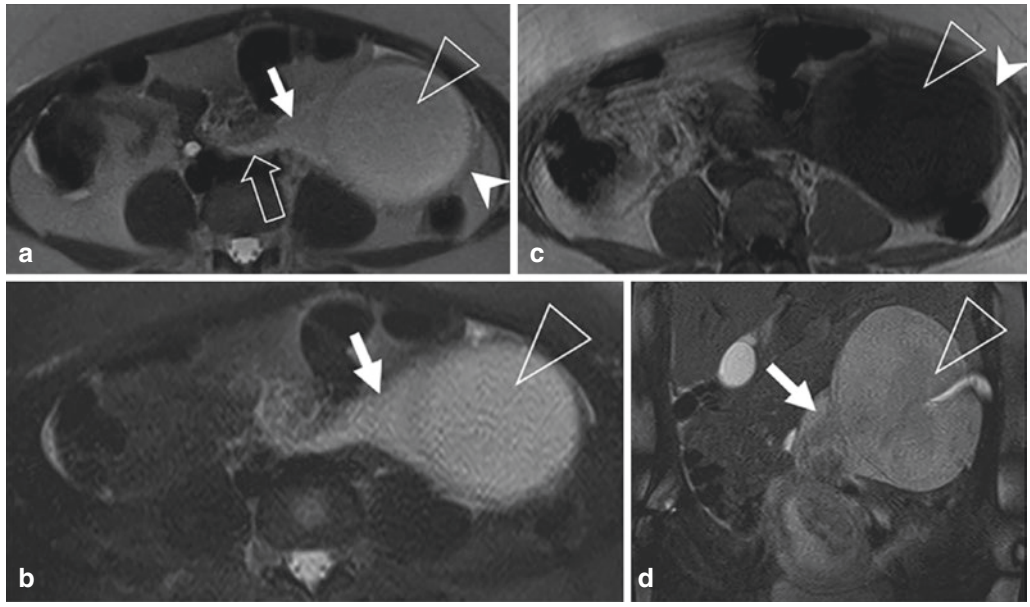

Fig. 11.8 Ovarian torsion in pregnancy—(**a**) T2-weighted, (**b**) T2-weighted FS, (**c**) T1-weighted, and (**d**) coronal T2-weighted FS MR images demonstrating a thickened and edematous vascular pedicle (white arrow), and a large simple cyst (open arrowhead) with mild wall thickening (arrowhead). Note the beaking and subtle swirled appearance of the vascular pedicle (open arrow)

setting of torsion [87]. Rotation of the pedicle results in vascular compromise, edema, and/or hemorrhage in the tube and the pedicle. The twist can be seen on US [88] and MR [79] and is described as the "whirlpool sign." Edema and hemorrhage cause enlargement of the tube and pedicle. The normal fallopian tube is less than 3 mm in diameter at its narrowest point [78], and up to 10 mm at the cornua or fimbriae. Asymmetric thickening of a fallopian tube should prompt close evaluation of the ipsilateral adnexa for additional signs of torsion. Tubal thickening is evident on T2-weighted images [15, 89] and may be more conspicuous on low *B*-value DWI because of its high T2 contrast [16]. Simple hydrosalpinx can look similar to a torsed tube, but identifying twisting or beaking [89] of the tube increases confidence in the diagnosis of torsion. A torsed fallopian tube may appear T1 hyperintense, due to development of hematosalpinx. Hemorrhagic infarction of the pedicle results in restricted diffusion, with curvilinear high DWI signal and low ADC signal [87, 90] extending from the uterine cornua to the ovary. Isolated tubal torsion can occur, but is extremely rare, and should be a diagnosis of exclusion. Tubal thickening and the "whirlpool" sign are the most specific and reliable signs of ovarian torsion, with diffusion restriction and tubal hemorrhage highly specific for hemorrhagic infarction [79] (Fig. 11.9).

Abnormal positioning of the ovary may indicate torsion, as rotation of the ovary around the pedicle causes deviation of the pelvic structures. The normal ovary tends to reside along the pelvic sidewall, near the iliac vessels, lateral and just superior to the uterine cornua. It can be located by following the gonadal veins inferiorly from the renal vein on the left or from the infrarenal inferior vena cava on the right. A torsed ovary commonly rotates to lie on top of the uterus or within the rectouterine pouch. Less commonly, a torsed ovary is located anterior to the uterus or in the contralateral pelvis [78, 80]. The uterus also deviates in torsion, with early reports of deviation ipsilateral to the torsed ovary [91, 92], but later reports showing ipsilateral and contralateral deviation [80, 87, 89]. In the majority of patients, the

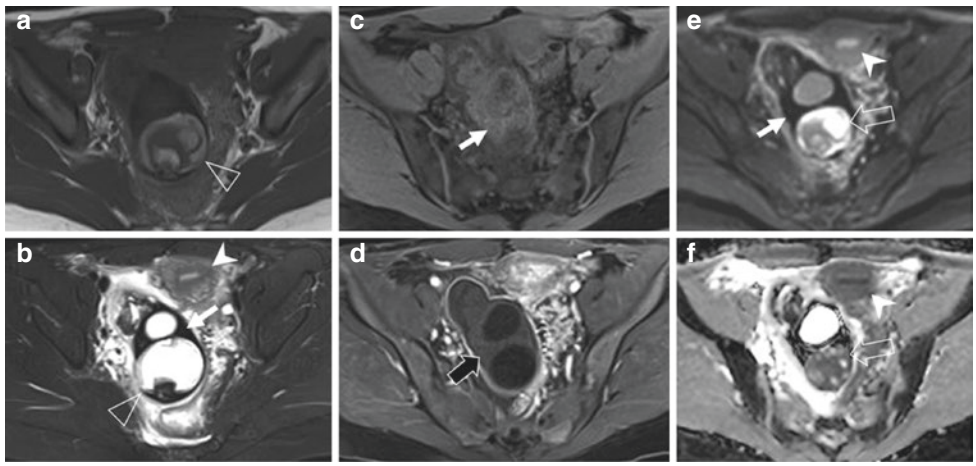

Fig. 11.9 Ovarian torsion with hemorrhagic infarction—(**a**) T2-weighted MR image demonstrating a cystic teratoma (open arrowhead) in an enlarged, eccentric, posteriorly positioned torsed ovary. (**b**) T2-weighted FS and (**c**) pre-contrast T1-weighted MR images showing thickened ovarian stroma (white arrow), with loss of T2 signal intensity and T1 signal hyperintensity compatible with hemorrhagic infarction of the stroma. (**d**) Post-contrast T1-weighted MR image shows no enhancement of the stroma (black arrow). (**e**) DWI and (**f**) ADC MR images show signal voids in the ovarian stroma (white arrow) indicating dephasing from blood products, and diffusion restriction within the teratoma (open arrow). Note the uterine deviation on multiple images (arrowhead)

ovary is in an atypical location, and the uterus is deviated from midline.

Asymmetric ovarian enlargement should prompt consideration of ovarian torsion. The measured ovary should include cysts or solid masses, and be compared to the contralateral ovary. Four centimeters is the upper limit of normal for maximum long-axis diameter of the ovary, although reproductive age women may have normal cysts measuring 5–7 cm, which can result in asymmetry of normal ovaries. The range of ovarian diameter in confirmed patients with torsion is 1–30 cm, with reported mean/median sizes of 8.7–13.5 cm [77, 78, 80]. Some investigators describe increased cross-sectional area or volume in torsion, with reported mean areas of 11.3–19 cm^2, and a range 3.8–50 cm^2 [79, 89].

Edema or hemorrhage in the ovarian stroma partially accounts for the enlargement of a torsed ovary. On T2-weighted MR imaging, normal ovarian stroma is isointense to skeletal muscle, with the stroma of torsed ovaries described as T2 hyperintense and T1 hypointense [89, 93] due to edema. Later investigations have suggested that stromal T2 signal is not sensitive or specific [79] for torsion, since malignancy and infection can result in T2 hyperintensity. Focal or diffuse T1 hyperintensity, DWI hyperintensity, and ADC hypointensity within the ovarian stroma have a poor prognosis and correlate with hemorrhagic infarction [15, 79, 87, 89, 90]. If the ADC values of ovarian stroma are below 1.8×10^{-3} mm^2/s, the sensitivity and specificity for hemorrhagic infarction is reportedly 88% and 100%, respectively [15]. The vast majority of torsed ovaries will demonstrate enhancement after intravenous gadolinium administration; however, a nonenhancing ovary has a poor prognosis, and hemorrhagic infarction and nonviability are common [87].

Cysts are present in up to 80% of torsed ovaries [78], and the walls of cysts within an ovary may develop abnormalities in the setting of torsion. The wall thickness of a normal ovarian follicle or hemorrhagic cyst is less than 3 mm, and has signal intensity similar to ovarian stroma. Edema or hemorrhage resulting from torsion results in wall thickening [78, 87, 91]. A thin T2 hypointense rim in the wall correlates with hemorrhagic infarction on histology and may carry a poor prognosis for the viability of the ovary [83]. Subacute hemorrhagic infarction results in a thin rim of T1 hyperintensity due to the presence of methemoglobin, but hyperacute and acute hemorrhage can be T1 iso- to hypointense, as oxy- and deoxyhemoglobin predominate in the early stages of hematoma formation [15]. Blood products with the wall of a cyst also result in DWI hyperintensity, and ADC hypointensity, and may indicate hemorrhage [87].

Ascites and periovarian fat stranding are common findings in torsion, but are often present in other acute processes presenting with abdominal or pelvic pain. Ascites is reported on CT and MR in most patients with ovarian torsion [78, 80, 87, 92], and while it has high sensitivity, its lack of specificity diminishes its usefulness in the diagnosis of torsion. Periovarian fat stranding is not present in most patients with ovarian torsion, but when present correlates with a nonviable ovary and the development of hemorrhagic infarction [78, 80].

11.4.4 Management

In the past, ovarian torsion was managed with salpingo-oophorectomy due to concerns that a necrotic ovary might lead to infection, that detorsion of the ovary could result in thromboembolism, and concern for underlying malignancy. Adnexal sparing surgery is now the preferred treatment option. Patients treated with detorsion do not have an increased incidence of pulmonary embolism, or increased morbidity and mortality, compared to those treated with oophorectomy [94, 95]. Even patients with "black-bluish" appearing ovaries at surgery had recovery of ovarian function and no increased morbidity when treated with detorsion [96, 97]. However, if an ovary is frankly necrotic due to delayed diagnosis of torsion, oophorectomy should be considered. When an ovarian cyst or benign ovarian neoplasm is present, cystectomy or cyst aspiration can be performed to reduce the potential for retorsion. Oophoropexy may also reduce the risk of retorsion and may be considered for prophylactic treatment of the contralateral ovary [98, 99].

Identification of hemorrhagic infarction in torsed ovaries is a focus in the radiology literature. It is not clear that the presence of hemorrhagic infarction indicates the ovary is nonviable, and additional studies are required before management decisions are made based on the MR findings of hemorrhage.

11.5 Ectopic Pregnancy

11.5.1 Background

Ectopic pregnancy refers to the implantation of an embryo outside of the uterine canal, which if untreated can result in maternal hemorrhage and death. The treatment and presentation of ectopic pregnancy differs based on the site of implantation. Ectopic pregnancy is most common in the fallopian tube [100], and as the gestational sac enlarges and increases in vascularity, there is increasing risk of tubal rupture, hemorrhage, and death. Less common sites of ectopic pregnancy include interstitial, abdominal, cervical, ovarian, and cesarean scar-related presentation [101]. The increased use of transvaginal sonography to confirm intrauterine pregnancy has led to earlier diagnosis of ectopic pregnancy [102]. Nonruptured ectopic pregnancy often presents with mild vaginal bleeding, crampy abdominal and pelvic pain, and positive HCG levels [103]. Ruptured ectopic pregnancy presents with hypotension, tachycardia, and rebound tenderness and may rapidly progress to death.

Transvaginal sonography should demonstrate a gestational sac when the estimated gestational age is 5.5 weeks, and when quantitative HCG is 1500–2500 mIU/mL. The absence of a gestational sac on ultrasound should be described as a pregnancy of unknown location [103, 104]. Transvaginal ultrasound is sensitive for ectopic pregnancy [105–107], but ectopic pregnancies can be mistaken for corpus luteal cysts, hemorrhagic cysts, ovarian neoplasms, pedunculated fibroids, bowel, and endometriomas. Sonographic diagnosis of pregnancy of unknown location is often managed with serial HCG levels and follow-up US in 2–7 days. If there is persistent pain and/or vaginal bleeding, MRI may be warranted to further characterize the etiology of pelvic pain, without additional delay in diagnosis.

11.5.2 Epidemiology

The incidence of ectopic pregnancy has been increasing over the past 4 decades, with the last comprehensive review by the U.S. Centers for Disease Control estimating that 2% of pregnancies are ectopic [108, 109]. As the incidence has risen, death related to ectopic pregnancy has fallen over 90%, now accounting for only 6% of maternal deaths [110–112]. Ectopic pregnancy requiring hospitalization has also fallen, with more than 50% of ectopic pregnancy treated in outpatient settings [109].

The predominant risk factors for ectopic pregnancy are related to abnormalities of the fallopian tube. Women with prior ectopic pregnancy, prior tubal surgery, or known tubal abnormality are at highest risk for ectopic pregnancy. Women with prior pelvic inflammatory disease, sexually transmitted infection, IUD, or subfertility/infertility have an intermediate risk for ectopic pregnancy. Ectopic pregnancy has a mild association with prior abdominal or pelvic surgery, smoking, early age of sexual intercourse, and multiple sexual partners. When the HCG level is positive, ultrasound fails to demonstrate an intrauterine gestation, and ectopic pregnancy is suspected, an MR can be used to distinguish ectopic pregnancy from other acute conditions including ovarian torsion, appendicitis, and pelvic inflammatory disease [113, 114].

11.5.3 MR Findings

Tubal ectopic pregnancy occurs most frequently in the ampulla of the fallopian tube. The ectopic gestational sac has been described on MR as a sac-like cystic structure in the adnexa but outside of the ovary [114]. The gestational sac tends to have a thick wall, and MR may demonstrate three distinct layers, described as a "3-ring"

appearance [115]. The wall may have focal hemorrhage or rim-like hemorrhage, evident by T1 intermediate to hyperintense signal, and corresponding T2 hypointensity. The wall will show marked enhancement, which is sometime "dot-like" or stippled [116]. The central portion of the gestational sac is often heterogeneous, with solid enhancing nodules, internal hemorrhage, fluid-fluid levels, or less likely simple fluid [115]. Hemorrhage within the sac is most commonly T1 intermediate to hyperintense and T2 hypointense, and may show loss of signal on T2*-weighted MR imaging [117]. The gestational sac size increases with increasing gestational age. Tubal ectopics present with a mean sac diameter of 4 cm [118]. Hematosalpinx is often present with tubal ectopic pregnancy. The fallopian tube will be dilated and contain T1 intermediate to hyperintense signal. There may be T2 heterogeneity and a fluid-fluid level in the tube. The wall of the fallopian tube may be slightly thickened and will show marked enhancement [8, 115–117] (Figs. 11.10 and 11.11).

Differentiation of a tubal ectopic pregnancy from a corpus luteal cyst can be challenging. A corpus luteal cyst is present in early pregnancy and has imaging features similar to an ectopic gestational sac. On MR, a corpus luteal cyst should have a smooth, convex, or mildly wavy thick wall. The wall is T1 intermediate to hyperintense and uniformly T2 hypointense, with uniform enhancement [116]. Intra- or extra-ovarian location is the best distinguishing factor. Corpus luteal cysts are always located within the ovary, and ovarian ectopic pregnancy is rare [100] (Fig. 11.12).

Nontubal ectopic pregnancy accounts for fewer than 5% of ectopic pregnancies [119], often present later than tubal ectopics, and have higher morbidity and mortality due to higher rate of rupture and delayed presentation. The gestational sac of nontubal ectopics has similar MR features, with a thick-walled, sac-like, hemorrhagic mass, and is distinguished from tubal ectopics by their rarity, location, and management.

Interstitial ectopics present when the gestational sac implants in the intrauterine portion of the

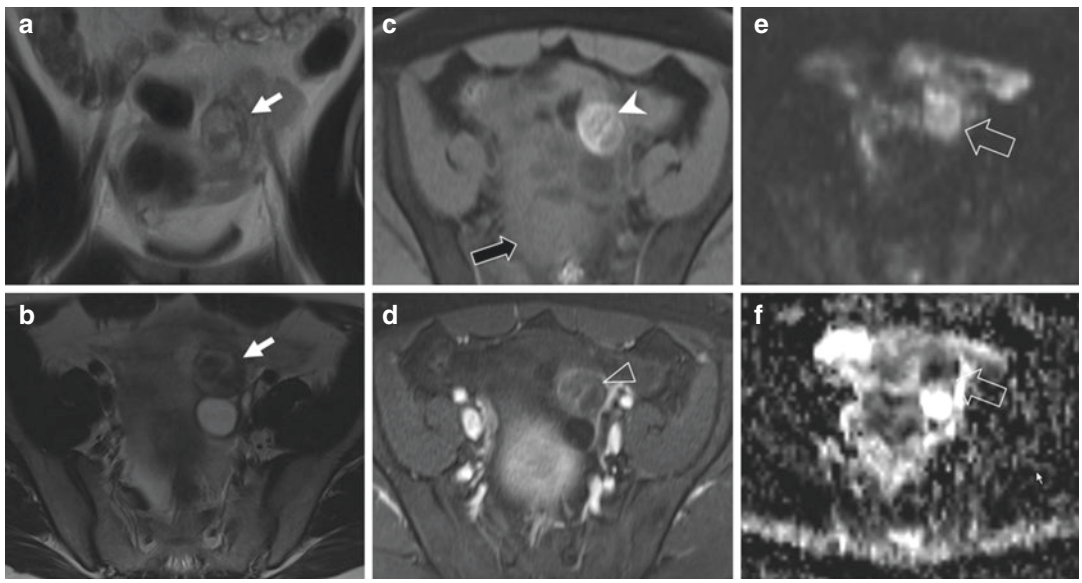

Fig. 11.10 Tubal ectopic pregnancy—(**a**) T2-weighted and (**b**) T2-weighted FS MR images demonstrating a complex adnexal mass (white arrow) in a woman with positive HCG level and no intrauterine gestation. (**c**) Pre-contrast T1-weighted MR image showing a hemorrhagic mass (arrowhead) and intraperitoneal hemorrhage (black arrow). (**d**) Post-contrast T1-weighted MR image showing mild stippled enhancement. (**e**) DWI and (**f**) ADC MR images showing diffusion restriction of the adnexal mass (open arrow). Surgery confirmed a ruptured tubal ectopic pregnancy

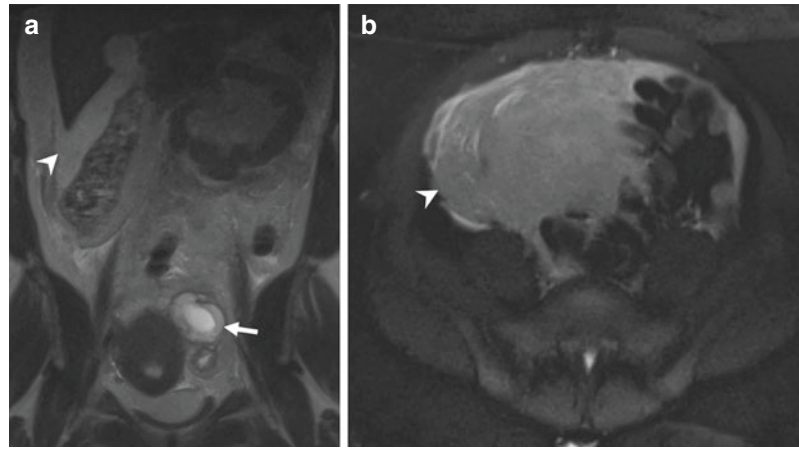

Fig. 11.11 Three-ring sign of tubal ectopic pregnancy—(**a**) coronal and (**b**) axial T2-weighted MR images demonstrate a tubal ectopic gestational sac (white arrow), with a thin hypointense outer ring, a thick hyperintense middle ring, and a thin hypointense inner ring. Note the large volume hemoperitoneum on both images (arrowhead)

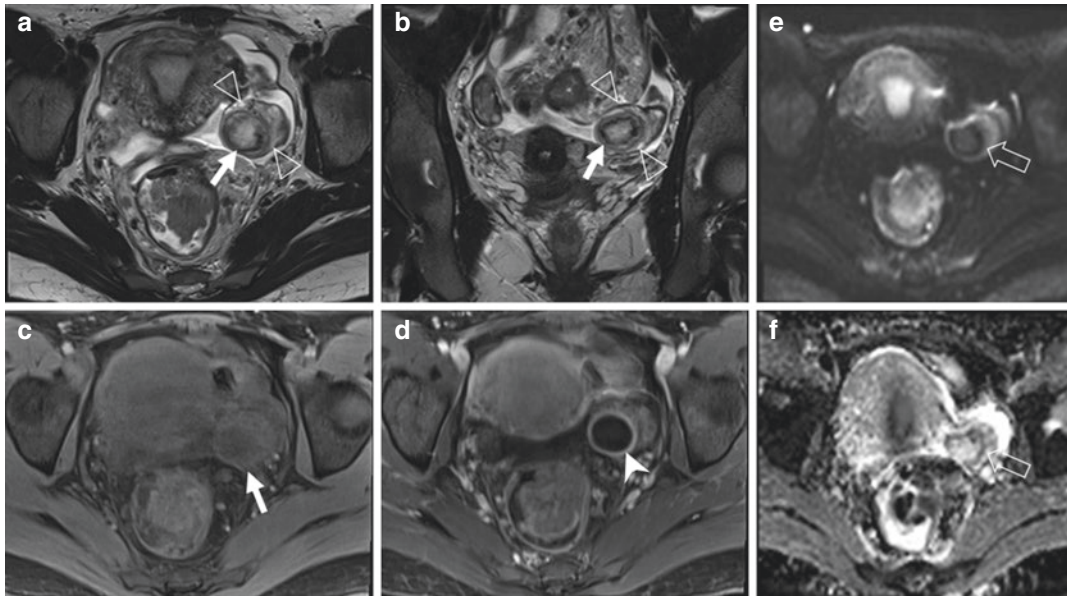

Fig. 11.12 Corpus luteal cyst—(**a**) axial and (**b**) coronal T2-weighted MR images demonstrate a corpus luteal cyst in the left ovary. Its location in the ovary is evident by a "claw sign" (open arrowheads) with ovarian stroma partially encompassing the cyst. Note the wavy hypointense rim (white arrow). (**c**) Pre-contrast T1 and (**d**) post-contrast T1-weighted MR images demonstrate smooth circumferential enhancement (arrowhead). The rim is hypointense on (**e**) DWI and (**f**) ADC (open arrow) indicating dephasing from blood products

fallopian tube, and is characterized by a gestational sac eccentrically located in or at the margin of the uterine cornua with less than 5 mm of surrounding myometrium [120, 121]. A closely related entity is cornual implantation, which is defined by implantation in the horn of a bicornuate uterus, and is similarly managed [122]. Cornual pregnancy may also refer to an eccentric implantation onto endometrium within the uterine cornua, and can be distinguished by a surrounding myometrial thickness of >5 mm (Figs. 11.13 and 11.14).

Abdominal ectopics are defined by implantation of the gestational sac on a peritoneal surface and can occur anywhere in the abdomen or pelvis. Abdominal pregnancy can be carried to term, but is at high risk for fetal demise from poor placental blood supply, and high risk for maternal demise from rupture [123–129].

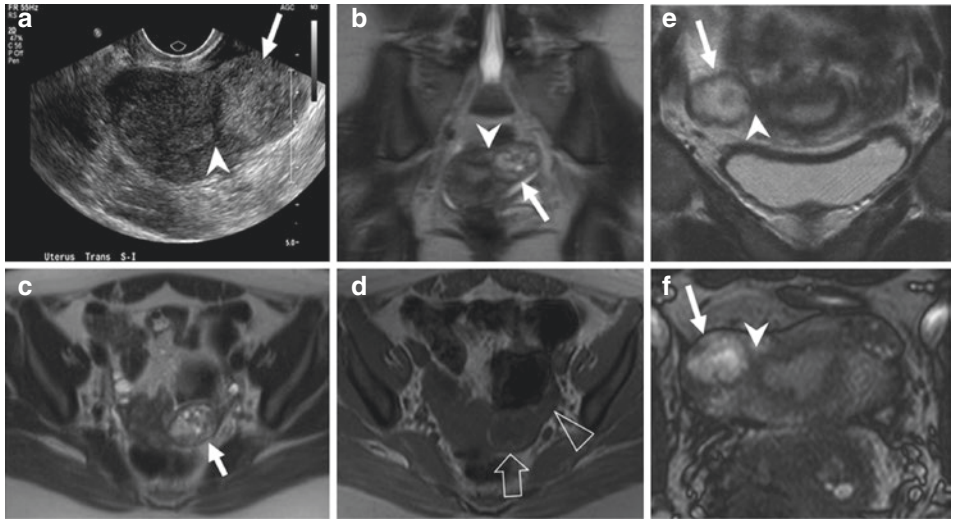

Fig. 11.13 Interstitial pregnancy—(**a**) US demonstrating a hyperechoic, heterogeneous ectopic pregnancy (white arrow) at the cornua (arrowhead) of the uterus in a women with positive HCG. (**b**) Coronal and (**c**) trans axial T2-weighted MR images demonstrate a heterogeneously T2 hyperintense ectopic (white arrow) at the junction of the uterine cornua and the fallopian tube (arrowhead). (**d**) T1-weighted MR image shows a hyperintense rim of hemorrhage (open arrow) along the margin of the ectopic and T1 hyperintense hemorrhage within the contiguous fallopian tube (open arrowhead). (**e**) Coronal T2-weighted and (**f**) axial SSFP MR images in a different patient with interstitial pregnancy demonstrate a heterogeneously T2 hyperintense ectopic (white arrow) at the uterine cornua (arrowhead). Both ectopic pregnancies were successfully treated with methotrexate

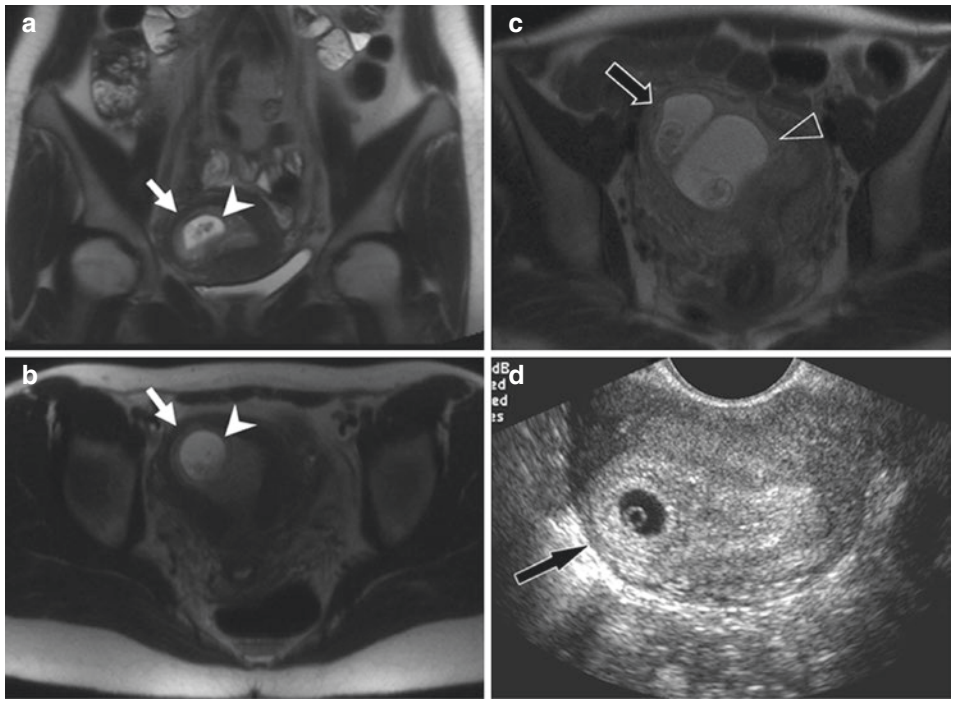

Fig. 11.14 Cornual pregnancy—(**a**) coronal and (**b**) axial T2-weighted MR images demonstrate an eccentric gestational sac in the uterine cornua with >5 mm of surrounding myometrium. (**c**) Axial T2 image in a different patient demonstrates a twin gestation, with one gestational sac located in the cornua of the uterus (black arrow), and one in the uterine body (open arrowhead). (**d**) US image shows the gestational sac in the uterine cornua. The cornual gestation was treated with selective reduction

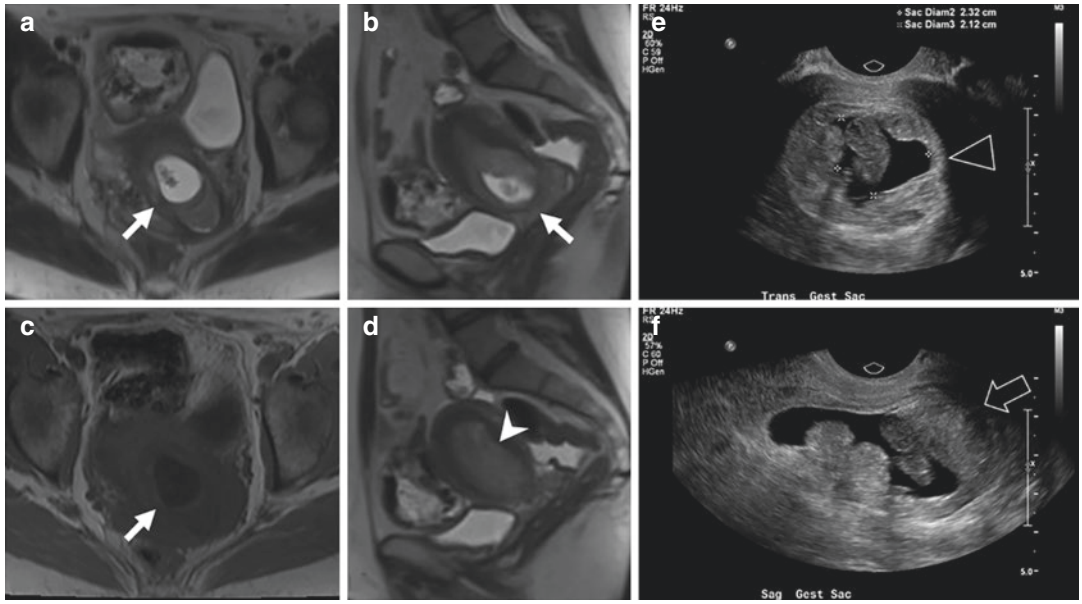

Fig. 11.15 Cervical pregnancy—(**a**) axial and (**b**) sagittal T2-weighted, and (**b**) T1-weighted MR images show a gestational sac located low in the endocervical canal (white arrow). (**d**) Sagittal T2-weighted MR image shows no gestational sac in the endouterine canal (arrowhead). (**e**) Transverse and (**f**) long axis transvaginal ultrasound images show a gestational sac and a fetal pole

Cervical pregnancy accounts for fewer than 1% of ectopic pregnancies and is predominately described in case reports and small case series. Cervical pregnancy typically presents with vaginal bleeding and can mimic spontaneous abortion or a cervical polyp, with the gestational sac located between the internal and external cervical os [130–133] (Fig. 11.15).

Ovarian ectopic pregnancies present a unique diagnostic challenge, as the gestation sac and a hemorrhagic corpus luteal cyst can be difficult to distinguish. Ovarian ectopic pregnancies have an association with an IUD [134]. The features of corpus luteal cyst and ectopic gestational sac described above may help distinguish an ovarian ectopic from a corpus luteal cyst.

Cesarean scar pregnancies have an increasing incidence in certain parts of the World, which is related to the increasing rate of cesarean section in North America. Diagnosis is made when a gestational sac is identified in the anterior lower uterine myometrium in a woman with prior cesarean section. Termination is recommended, although there are case reports of expectant management and early cesarean section [135–137].

11.5.4 Management

Ectopic pregnancy is preferably treated with single dose of systemic methotrexate, with greater than 90% success rate in select patient populations [138]. Methotrexate therapy is commonly offered to hemodynamically stable women, with an HCG level less than 5000 mIU/mL, a gestational sac smaller than 4 cm, no contraindication to methotrexate, and a willingness to follow-up for serial evaluation [139]. Failure of systemic therapy occurs more often in patients with high HCG levels (5000–10,000) and fetal cardiac activity [140].

Multidose therapy, local methotrexate injection, and local KCl injection have been proposed after single dose failure or in patients with fetal cardiac activity, high HCG levels, or late presentation [139, 141]. Surgical therapy is required for unstable patients, patients with evidence of rupture, or those who fail medical therapy. The presence of a small volume of hemorrhage confined to the pelvis is not a contraindication to medical therapy, as small volume hemorrhage is commonly seen with nonruptured tubal ectopics

[140, 142, 143]. Hemorrhage which extends into the paracolic gutters and abdomen may indicate tubal rupture and require emergent surgery.

Imaging follow-up after medical treatment is not routinely indicated. If follow-up imaging is obtained, the ectopic pregnancy often enlarges, prior to normalization of HCG levels. Mean ectopic enlargement on US is reportedly 6 cm. Sixty-nine percent of residual ectopics resolved with HCG normalization, but many patients will have residual complex masses after HCG normalization. Mean time to resolution of the ectopic is reportedly 44 days (range 25–63), when it persists beyond HCG normalization [118].

Conclusion

MR imaging can function as a primary or secondary imaging modality for the evaluation of acute pelvic pain. Most often, acute pelvic pain is evaluated with ultrasound or CT, and indeterminate or complex findings prompt MR imaging. Pelvic MR can be performed at 1.5 T or 3 T, with or without intravenous gadolinium, and with optimal sequence selection should take 30 min or less. Single-shot T2-weighted imaging is the foundation of any pelvic MR examination and should be done in multiple planes. Infection is often evident by parametrial stranding, thickening of the round ligament and uterosacral ligament, tubal enlargement and wall thickening, and inflammatory cystic adnexal masses. Ovarian torsion should be suspected when the ovary is asymmetrically enlarged, abnormally positioned, and is accompanied by thickening of the vascular pedicle. Ectopic pregnancies are circumscribed hypervascular masses with internal heterogeneity, which are most commonly located in the fallopian tube. MR utilization continues to rise, and familiarity with acute MR findings is an increasingly important part of effective emergency radiology and body imaging.

References

1. Lazarus E, Mayo-Smith WW, Mainiero MB, Spencer PK. CT in the evaluation of nontraumatic abdominal pain in pregnant women. Radiology. 2007;244(3):784–90.
2. Nagayama M, Watanabe Y, Okumura A, Amoh Y, Nakashita S, Dodo Y, Fast MR. Imaging in obstetrics. Radiographics. 2002;22(3):563–80.
3. Leyendecker JR, Gorengaut V, Brown JJ. MR imaging of maternal diseases of the abdomen and pelvis during pregnancy and the immediate postpartum period. Radiographics. 2004;24(5):1301–16.
4. Singh A, Danrad R, Hahn PF, Blake MA, Mueller PR, Novelline R. MR imaging of the acute abdomen and pelvis: acute appendicitis and beyond. Radiographics. 2007;27(5):1419–31.
5. Heverhagen JT, Klose KJ. MR imaging for acute lower abdominal and pelvic pain. Radiographics. 2009;29(6):1781–96.
6. Qayyum A. Diffusion-weighted imaging in the abdomen and pelvis: concepts and applications. Radiographics. 2009;29(6):1797–810.
7. Lubarsky M, Kalb B, Sharma P, Keim SM, Martin DR. MR imaging for acute nontraumatic abdominopelvic pain: rationale and practical considerations. Radiographics. 2013;33(2):313–37.
8. Kataoka M, Kido A, Koyama T, Isoda H, Umeoka S, Tamai K, et al. MRI of the female pelvis at 3T compared to 1.5T: evaluation on high-resolution T2-weighted and HASTE images. J Magn Reson Imaging. 2007;25(3):527–34.
9. Choi SH, Kim SH, Choi HJ, Park BK, Lee HJ. Preoperative magnetic resonance imaging staging of uterine cervical carcinoma: results of prospective study. J Comput Assist Tomogr. 2004;28(5):620–7.
10. Johnson AK, Filippi CG, Andrews T, Higgins T, Tam J, Keating D, et al. Ultrafast 3-T MRI in the evaluation of children with acute lower abdominal pain for the detection of appendicitis. Am J Roentgenol. 2012;198(6):1424–30.
11. Expert Panel on MR Safety, Kanal E, Barkovich AJ, Bell C, Borgstede JP, Bradley WG, et al. ACR guidance document on MR safe practices: 2013. J Magn Reson Imaging. 2013;37(3):501–30.
12. ACR Manual on Contrast Media v10.2. American College of Radiology; 2016
13. Thomsen HS, Morcos SK, Almén T, Bellin M, Bertolotto M, Bongartz G, et al. Nephrogenic systemic fibrosis and gadolinium-based contrast media: updated ESUR Contrast Medium Safety Committee guidelines. Eur Radiol. 2013;23(2):307–18.
14. Li W, Zhang Y, Cui Y, Zhang P, Wu X. Pelvic inflammatory disease: evaluation of diagnostic accuracy with conventional MR with added diffusion-weighted imaging. Abdom Imaging. 2013;38(1):193–200.
15. Kato H, Kanematsu M, Uchiyama M, Yano R, Furui T, Morishige K. Diffusion-weighted imaging of ovarian torsion: usefulness of apparent diffusion coefficient (ADC) values for the detection of hemorrhagic infarction. Magn Reson Med Sci. 2014;13(1):39–44.

16. Fujii S. Diffusion-weighted imaging findings of adnexal torsion: initial results. Eur J Radiol. 2011;77:330–4.
17. Eschenbach DA, Wölner-Hanssen P, Hawes SE, Pavletic A, Paavonen J, Holmes KK. Acute pelvic inflammatory disease: associations of clinical and laboratory findings with laparoscopic findings. Obstet Gynecol. 1997;89(2):184–92.
18. Brunham RC, Gottlieb SL, Paavonen J. Pelvic inflammatory disease. N Engl J Med. 2015;372(21):2039–48.
19. Monif GR. Clinical staging of acute bacterial salpingitis and its therapeutic ramifications. Am J Obstet Gynecol. 1982;143(5):489–95.
20. Soper DE. Pelvic inflammatory disease. Obstet Gynecol. 2010;116(2 Part 1):419–28.
21. Fitz-Hugh T. Acute gonococcic perihepatitis, a new syndrome of right upper quadrant abdominal pain in young women. Rev Gastroenterol. 1936;3:125–31.
22. Pickhardt PJ, Fleishman MJ, Fisher AJ. Fitz-Hugh–Curtis syndrome: multidetector CT Findings of transient hepatic attenuation difference and gallbladder wall thickening. Am J Roentgenol. 2003;180(6):1605–6.
23. Lee MH, Moon MH, Sung CK, Woo H, Oh S. CT findings of acute pelvic inflammatory disease. Abdom Imaging. 2014;39(6):1350–5.
24. Kreisel K. Prevalence of pelvic inflammatory disease in sexually experienced women of reproductive age—United States, 2013–2014. MMWR Morb Mortal Wkly Rep [Internet]. 2017 [cited 2017 May 16];66. http://www.cdc.gov/mmwr/volumes/66/wr/mm6603a3.htm
25. Sutton MY, Sternberg M, Zaidi A, St Louis ME, Markowitz LE. Trends in pelvic inflammatory disease hospital discharges and ambulatory visits, United States, 1985–2001. Sex Transm Dis. 2005;32(12):778–84.
26. Bohm MK, Newman L, Satterwhite CL, Tao G, Weinstock HS. Pelvic inflammatory disease among privately insured women, United States, 2001–2005. Sex Transm Dis. 2010;37(3):131–6.
27. Scholes D, Stergachis A, Heidrich FE, Andrilla H, Holmes KK, Stamm WE. Prevention of pelvic inflammatory disease by screening for cervical chlamydial infection. N Engl J Med. 1996;334(21):1362–6.
28. Brunham RC, Paavonen J, Stevens CE, Kiviat N, Kuo C-C, Critchlow CW, et al. Mucopurulent cervicitis—the ignored counterpart in women of urethritis in men. N Engl J Med. 1984;311(1):1–6.
29. Taylor SN, Lensing S, Schwebke J, Lillis R, Mena LA, Nelson AL, et al. Prevalence and treatment outcome of cervicitis of unknown etiology. Sex Transm Dis. 2013;40(5):379–85.
30. Imaoka I, Wada A, Matsuo M, Yoshida M, Kitagaki H, Sugimura K. MR imaging of disorders associated with female infertility: use in diagnosis, treatment, and management. Radiographics. 2003;23(6):1401–21.
31. Okamoto Y, Tanaka YO, Nishida M, Tsunoda H, Yoshikawa H, Itai YMR. Imaging of the uterine cervix: imaging-pathologic correlation. Radiographics. 2003;23(2):425–45.
32. Yitta S, Hecht EM, Mausner EV, Bennett GL. Normal or abnormal? Demystifying uterine and cervical contrast enhancement at multidetector CT. Radiographics. 2011;31(3):647–61.
33. Dohke M, Watanabe Y, Okumura A, Amoh Y, Hayashi T, Yoshizako T, et al. Comprehensive MR imaging of acute gynecologic diseases. Radiographics. 2000;20(6):1551–66.
34. Siddall KA, Rubens DJ. Multidetector CT of the female pelvis. Radiol Clin North Am. 2005;43(6):1097–118.
35. Paavonen J, Critchlow CW, DeRouen T, Stevens CE, Kiviat N, Brunham RC, et al. Etiology of cervical inflammation. Am J Obstet Gynecol. 1986;154(3):556–64.
36. Saini S, Kanetkar SR. Histopathol study lesions uterine cervix [Internet]. 2016 Dec 26 [cited 2017 May 17];(95463). http://www.jebmh.com/latest-articles.php?at_id=95463
37. Wager GP, Martin DH, Koutsky L, Eschenbach DA, Daling JR, Chiang WT, et al. Puerperal infectious morbidity: relationship to route of delivery and to antepartum Chlamydia trachomatis infection. Am J Obstet Gynecol. 1980;138(7):1028–33.
38. Watts DH, Eschenbach DA, Kenny GE. Early postpartum endometritis: the role of bacteria, genital mycoplasmas, and chlamydia trachomatis. Obstet Gynecol. 1989;73(1):52–60.
39. Cicinelli E, Matteo M, Tinelli R, Lepera A, Alfonso R, Indraccolo U, et al. Prevalence of chronic endometritis in repeated unexplained implantation failure and the IVF success rate after antibiotic therapy. Hum Reprod. 2015;30(2):323–30.
40. Nalaboff KM, Pellerito JS, Ben-Levi E. Imaging the endometrium: disease and normal variants. Radiographics. 2001;21(6):1409–24.
41. Sudderuddin S, Helbren E, Telesca M, Williamson R, Rockall A. MRI appearances of benign uterine disease. Clin Radiol. 2014;69(11):1095–104.
42. Jung SI, Kim YJ, Park HS, Jeon HJ, Jeong KA. Acute pelvic inflammatory disease: diagnostic performance of CT. J Obstet Gynaecol Res. 2011;37(3):228–35.
43. Revzin MV, Mathur M, Dave HB, Macer ML, Spektor M. Pelvic inflammatory disease: multimodality imaging approach with clinical-pathologic correlation. Radiographics. 2016;36(5):1579–96.
44. Patton DL, Moore DE, Spadoni LR, Soules MR, Halbert SA, Wang SP. A comparison of the fallopian tube's response to overt and silent salpingitis. Obstet Gynecol. 1989;73(4):622–30.
45. Kim MY, Rha SE, Soon Nam O, Jung SE, Lee YJ, Kim YS, et al. MR imaging findings of hydrosalpinx: a comprehensive review. Radiographics. 2009;29(2):495–507.
46. Propeck PA, Scanlan KA. Isolated fallopian tube torsion. Am J Roentgenol. 1998;170(4):1112–3.
47. Gross M, Blumstein SL, Chow LC. Isolated fallopian tube torsion: a rare twist on a common theme. Am J Roentgenol. 2005;185(6):1590–2.

48. Landers DV, Sweet RL. Current trends in the diagnosis and treatment of tuboovarian abscess. Am J Obstet Gynecol. 1985;151(8):1098–110.
49. Ueda H, Togashi K, Kataoka ML, Koyama T, Fujiwara T, Fujii S, et al. Adnexal masses caused by pelvic inflammatory disease: MR appearance. Magn Reson Med Sci. 2002;1(4):207–15.
50. Tukeva TA, Aronen HJ, Karjalainen PT, Molander P, Paavonen T, Paavonen J. MR imaging in pelvic inflammatory disease: comparison with laparoscopy and US. Radiology. 1999;210(1):209–16.
51. Rezvani M, Shaaban AM. Fallopian tube disease in the nonpregnant patient. Radiographics. 2011;31(2):527–48.
52. Ha HK, Lim GY, Cha ES, Lee HG, Ro HJ, Kim HS, et al. MR imaging of tubo-ovarian abscess. Acta Radiol 1987. 1995;36(5):510–4.
53. Twickler DM, Setiawan AT, Evans RS, Erdman WA, Stettler RW, Brown CE, et al. Imaging of puerperal septic thrombophlebitis: prospective comparison of MR imaging, CT, and sonography. Am J Roentgenol. 1997;169(4):1039–43.
54. Kubik-Huch RA, Hebisch G, Huch R, Hilfiker P, Debatin JF, Krestin GP. Role of duplex color Doppler ultrasound, computed tomography, and MR angiography in the diagnosis of septic puerperal ovarian vein thrombosis. Abdom Imaging. 1999;24(1):85–91.
55. Sharma P, Abdi S. Ovarian vein thrombosis. Clin Radiol. 2012;67(9):893–8.
56. Cuyper K, Eyselbergs M, Bernard P, Clabout L, Vanhoenacker FM. Added value of diffusion weighted MRI in the diagnosis of postpartum ovarian vein thrombosis. J Belg Soc Radiol [Internet]. 2014 [cited 2017 May 23];97(4). http://www.jbsr.be/articles/abstract/10.5334/jbr-btr.86/
57. Valicenti JF, Pappas AA, Graber CD, Williamson HO, Willis NF. Detection and prevalence of IUD-associated Actinomyces colonization and related morbidity. A prospective study of 69,925 cervical smears. JAMA. 1982;247(8):1149–52.
58. Chatwani A, Amin-Hanjani S. Incidence of actinomycosis associated with intrauterine devices. J Reprod Med. 1994;39(8):585–7.
59. Perlow JH, Wigton T, Yordan EL, Graham J, Wool N, Wilbanks GD. Disseminated pelvic actinomycosis presenting as metastatic carcinoma: association with the progestasert intrauterine device. Rev Infect Dis. 1991;13(6):1115–9.
60. Hawnaur JM, Reynolds K, McGettigan C. Magnetic resonance imaging of actinomycosis presenting as pelvic malignancy. Br J Radiol. 1999;72(862):1006–11.
61. Bae JH, Song R, Lee A, Park JS, Kim MR. Computed tomography for the preoperative diagnosis of pelvic actinomycosis. J Obstet Gynaecol Res. 2011;37(4):300–4.
62. O'Connor KF, Bagg MN, Croley MR, Schabel SI. Pelvic actinomycosis associated with intrauterine devices. Radiology. 1989;170(2):559–60.
63. Kim SH, Kim SH, Yang DM, Kim KA. Unusual causes of tubo-ovarian abscess: CT and MR imaging findings. Radiographics. 2004;24(6):1575–89.
64. Dejanović D, Ahnlide JA, Nilsson C, Berthelsen AK, Loft A. Pelvic actinomycosis associated with an intrauterine contraceptive device demonstrated on F-18 FDG PET/CT. Diagnostics. 2015;5(3):369–71.
65. Ness RB, Soper DE, Holley RL, Peipert J, Randall H, Sweet RL, et al. Effectiveness of inpatient and outpatient treatment strategies for women with pelvic inflammatory disease: results from the pelvic inflammatory disease evaluation and clinical health (peach) randomized trial. Am J Obstet Gynecol. 2002;186(5):929–37.
66. Pelvic Inflammatory Disease (PID)—2015 STD Treatment Guidelines [Internet]. [cited 2017 May 23]. https://www.cdc.gov/std/tg2015/pid.htm
67. Farid H, Lau TC, Karmon AE, Styer AK. Clinical characteristics associated with antibiotic treatment failure for tuboovarian abscesses. Infect Dis Obstet Gynecol. 2016;2016:e5120293.
68. Perez-Medina T, Huertas MA, Bajo JM. Early ultrasound-guided transvaginal drainage of tuba-ovarian abscesses: a randomized study. Ultrasound Obstet Gynecol. 1996;7(6):435–8.
69. Goharkhay N, Verma U, Maggiorotto F.Comparison of CT- or ultrasound-guided drainage with concomitant intravenous antibiotics vs. intravenous antibiotics alone in the management of tubo-ovarian abscesses. Ultrasound Obstet Gynecol. 2007;29(1):65–9.
70. Gjelland K, Ekerhovd E, Granberg S. Transvaginal ultrasound-guided aspiration for treatment of tubo-ovarian abscess: a study of 302 cases. Am J Obstet Gynecol. 2005;193(4):1323–30.
71. Labropoulos N, Malgor RD, Comito M, Gasparis AP, Pappas PJ, Tassiopoulos AK. The natural history and treatment outcomes of symptomatic ovarian vein thrombosis. J Vasc Surg Venous Lymphat Disord. 2015;3(1):42–7.
72. Taga S. Diagnosis and therapy of pelvic actinomycosis. J Obstet Gynaecol Res. 2007;33(6):882–5.
73. Smego RA, Foglia G. Actinomycosis. Clin Infect Dis. 1998;26(6):1255–61.
74. Lippes J. Pelvic actinomycosis: a review and preliminary look at prevalence. Am J Obstet Gynecol. 1999;180(2):265–9.
75. Garner JP, Macdonald M, Kumar PK. Abdominal actinomycosis. Int J Surg. 2007;5(6):441–8.
76. Hibbard LT. Adnexal torsion. Am J Obstet Gynecol. 1985;152(4):456–61.
77. Houry D, Abbott JT. Ovarian torsion: a fifteen-year review. Ann Emerg Med. 2001;38(2):156–9.
78. Hiller N, Appelbaum L, Simanovsky N, Lev-Sagi A, Aharoni D, Sella TCT. Features of adnexal torsion. Am J Roentgenol. 2007;189(1):124–9.
79. Béranger-Gibert S, Sakly H, Ballester M, Rockall A, Bornes M, Bazot M, et al. Diagnostic value of MR imaging in the diagnosis of adnexal torsion. Radiology. 2015;279(2):461–70.

80. Chiou S-Y, Lev-Toaff AS, Masuda E, Feld RI, Bergin D. Adnexal torsion. J Ultrasound Med. 2007;26(10):1289–301.
81. Duigenan S, Oliva E, Lee SI. Ovarian torsion: diagnostic features on CT and MRI with pathologic correlation. Am J Roentgenol. 2012;198(2): W122–31.
82. Fahmy HS, Swamy N, Elshahat HM. Revisiting the role of MRI in gynecological emergencies: an institutional experience. Egypt J Radiol Nucl Med. 2015;46(3):769–79.
83. Petkovska I, Duke E, Martin DR, Irani Z, Geffre CP, Cragun JM, et al. MRI of ovarian torsion: correlation of imaging features with the presence of perifollicular hemorrhage and ovarian viability. Eur J Radiol. 2016;85(11):2064–71.
84. Yuk J-S, Kim LY, Shin J-Y, Choi DY, Kim TY, Lee JHA. national population-based study of the incidence of adnexal torsion in the Republic of Korea. Int J Gynecol Obstet. 2015;129(2):169–70.
85. Mashiach S, Bider D, Moran O, Goldenberg M, Ben-Rafael Z. Adnexal torsion of hyperstimulated ovaries in pregnancies after gonadotropin therapy. Fertil Steril. 1990;53(1):76–80.
86. Ginath S, Shalev A, Keidar R, Kerner R, Condrea A, Golan A, et al. Differences between adnexal torsion in pregnant and nonpregnant women. J Minim Invasive Gynecol. 2012;19(6):708–14.
87. Moribata Y, Kido A, Yamaoka T, Mikami Y, Himoto Y, Kataoka M, et al. MR imaging findings of ovarian torsion correlate with pathological hemorrhagic infarction. J Obstet Gynaecol Res. 2015;41(9):1433–9.
88. Lee EJ, Kwon HC, Joo HJ, Suh JH, Fleischer AC. Diagnosis of ovarian torsion with color Doppler sonography: depiction of twisted vascular pedicle. J Ultrasound Med. 1998;17(2):83–9.
89. Ghossain MA, Hachem K, Buy J-N, Hourany-Rizk RG, Aoun NJ, Haddad-Zebouni S, et al. Adnexal torsion: magnetic resonance findings in the viable adnexa with emphasis on stromal ovarian appearance. J Magn Reson Imaging. 2004;20(3):451–62.
90. Fujii S, Kaneda S, Kakite S, Kanasaki Y, Matsusue E, Harada T, et al. Diffusion-weighted imaging findings of adnexal torsion: initial results. Eur J Radiol. 2011;77(2):330–4.
91. Rha SE, Byun JY, Jung SE, Jung JI, Choi BG, Kim BS, et al. CT and MR imaging features of adnexal torsion. Radiographics. 2002;22(2):283–94.
92. Kimura I, Togashi K, Kawakami S, Takakura K, Mori T, Konishi J. Ovarian torsion: CT and MR imaging appearances. Radiology. 1994;190(2):337–41.
93. Haque TL, Togashi K, Kobayashi H, Fujii S, Konishi J. Adnexal torsion: MR imaging findings of viable ovary. Eur Radiol. 2000;10(12):1954–7.
94. Zweizig S, Perron J, Grubb D, Mishell DR. Conservative management of adnexal torsion. Am J Obstet Gynecol. 1993;168(6):1791–5.
95. McGovern PG, Noah R, Koenigsberg R, Little AB. Adnexal torsion and pulmonary embolism: case report and review of the literature. Obstet Gynecol Surv. 1999;54(9):601–8.
96. Oelsner G, Bider D, Goldenberg M, Admon D, Mashiach S. Long-term follow-up of the twisted ischemic adnexa managed by detorsion. Fertil Steril. 1993;60(6):976–9.
97. Galinier P, Carfagna L, Delsol M, Ballouhey Q, Lemasson F, Le Mandat A, et al. Ovarian torsion. Management and ovarian prognosis: a report of 45 cases. J Pediatr Surg. 2009;44(9):1759–65.
98. Germain M, Rarick T, Robins E. Management of intermittent ovarian torsion by laparoscopic oophoropexy. Obstet Gynecol. 1996;88(4):715–7.
99. Grunewald B, Keating J, Brown S. Asynchronous ovarian torsion: the case for prophylactic oophoropexy. Postgrad Med J. 1993;69(810):318–9.
100. Breen JL. A 21 year survey of 654 ectopic pregnancies. Am J Obstet Gynecol. 1970;106(7):1004–19.
101. Körolu M, Kayhan A, Soylu FN, Erol B, Schmidtannwald C, Gürses C, et al. MR imaging of ectopic pregnancy with an emphasis on unusual implantation sites. Jpn J Radiol. 2013;31(2):75–80.
102. Cacciatore B, Stenman U-H, Ylostalo P. Early screening for ectopic pregnancy in high-risk symptom-free women. Lancet. 1994;343(8896):517–8.
103. Barnhart KT. Ectopic pregnancy. N Engl J Med. 2009;361(4):379–87.
104. Kirk E, Bottomley C, Bourne T. Diagnosing ectopic pregnancy and current concepts in the management of pregnancy of unknown location. Hum Reprod Update. 2014;20(2):250–61.
105. Barnhart K, Mennuti MT, Benjamin I, Jacobson S, Goodman D, Coutifaris C. Prompt diagnosis of ectopic pregnancy in an emergency department setting. Obstet Gynecol. 1994;84(6):1010–5.
106. Condous G, Lu C, Van Huffel SV, Timmerman D, Bourne T. Human chorionic gonadotrophin and progesterone levels in pregnancies of unknown location. Int J Gynecol Obstet. 2004;86(3):351–7.
107. Shalev E, Yarom I, Bustan M, Weiner E, Ben-Shlomo I. Transvaginal sonography as the ultimate diagnostic tool for the management of ectopic pregnancy: experience with 840 cases. Fertil Steril. 1998;69(1):62–5.
108. Goldner TE, Lawson HW, Xia Z, Atrash HK. Surveillance for ectopic pregnancy—United States, 1970–1989. MMWR CDC Surveill Summ Morb Mortal Wkly Rep CDC Surveill Summ. 1993;42(6):73–85.
109. Centers for Disease Control. Current trends ectopic pregnancy: United States, 1990–1992. MMWR Wkly. 1995;44(3):46–8.
110. Chang J, Elam-Evans LD, Berg CJ, Herndon J, Flowers L, Seed KA, et al. Pregnancy-related mortality surveillance—United States, 1991–1999. MMWR Surveill Summ. 2003;52(2):1–8.
111. Grimes DA. Estimation of pregnancy-related mortality risk by pregnancy outcome, United States, 1991 to 1999. Am J Obstet Gynecol. 2006; 194(1):92–4.

112. Creanga AA, Shapiro-Mendoza CK, Bish CL, Zane S, Berg CJ, Callaghan WM. Trends in ectopic pregnancy mortality in the United States: 1980–2007. Obstet Gynecol. 2011;117(4):837–43.
113. Tamai K, Koyama T, Saga T, Kido A, Kataoka M, Umeoka S, et al. MR features of physiologic and benign conditions of the ovary. Eur Radiol. 2006;16(12):2700–11.
114. Tamai K, Koyama T, Togashi K. MR features of ectopic pregnancy. Eur Radiol. 2007;17(12): 3236–46.
115. Si M-J, Gui S, Fan Q, Han H-X, Zhao Q-Q, Li Z-X, et al. Role of MRI in the early diagnosis of tubal ectopic pregnancy. Eur Radiol. 2016;26(7):1971–80.
116. Takahashi A, Takahama J, Marugami N, Takewa M, Itoh T, Kitano S, et al. Ectopic pregnancy: MRI findings and clinical utility. Abdom Imaging. 2013;38(4):844–50.
117. Yoshigi J, Yashiro N, Kinoshita T, O'uchi T, Kitagaki H. Diagnosis of ectopic pregnancy with MRI: efficacy of T2-weighted imaging. Magn Reson Med Sci. 2006;5(1):25–32.
118. Gamzu R, Almog B, Levin Y, Pauzner D, Lessing JB, Jaffa A, et al. The ultrasonographic appearance of tubal pregnancy in patients treated with methotrexate. Hum Reprod. 2002;17(10):2585–7.
119. Bouyer J, Coste J, Fernandez H, Pouly JL, Job-Spira N. Sites of ectopic pregnancy: a 10 year population-based study of 1800 cases. Hum Reprod. 2002;17(12):3224–30.
120. Filhastre M, Dechaud H, Lesnik A, Taourel P. Interstitial pregnancy: role of MRI. Eur Radiol. 2005;15(1):93–5.
121. Bourdel N, Roman H, Gallot D, Lenglet Y, Dieu V, Juillard D, et al. Interstitial pregnancy. Ultrasonographic diagnosis and contribution of MRI. A case report. Gynécologie Obstétrique Fertil. 2007;35(2):121.
122. Moawad NS, Mahajan ST, Moniz MH, Taylor SE, Hurd WW. Current diagnosis and treatment of interstitial pregnancy. Am J Obstet Gynecol. 2010;202(1):15–29.
123. Cohen J, Weinreb J, Lowe T, Brown CMR. imaging of a viable full-term abdominal pregnancy. Am J Roentgenol. 1985;145(2):407–8.
124. Wagner A, Burchardt A-JMR. Imaging in advanced abdominal pregnancy a case report of fetal death. Acta Radiol. 1995;36(2):193–5.
125. Malian V, Lee JE. MR imaging and MR angiography of an abdominal pregnancy with placental infarction. Am J Roentgenol. 2001;177(6):1305–6.
126. Ozdemir I, Demirci F, Yucel O, Alper M. Primary omental pregnancy presenting with hemorrhagic shock. Gynecol Obstet Invest. 2003;55(2):116–8.
127. Wong WC, Wong BPY, Kun KY, Ng TK, Kwok SY, Lee CK. Primary omental ectopic pregnancy. J Obstet Gynaecol Res. 2004;30(3):226–9.
128. Børlum K-G, Blom R. Primary hepatic pregnancy. Int J Gynecol Obstet. 1988;27(3):427–9.
129. Cormio G, Santamato S, Vimercati A, Selvaggi L. Primary splenic pregnancy. A case report. J Reprod Med. 2003;48(6):479–81.
130. Werber J, Prasadarao PR, Harris VJ. Cervical pregnancy diagnosed by ultrasound. Radiology. 1983;149(1):279–80.
131. Jung SE, Byun JY, Lee JM, Choi BG, Hahn ST, Characteristic MR findings of cervical pregnancy. J Magn Reson Imaging. 2001;13(6):918–22.
132. Gun M, Mavrogiorgis M. Cervical ectopic pregnancy: a case report and literature review. Ultrasound Obstet Gynecol. 2002;19(3):297–301.
133. Sherer DM, Gorelick C, Dalloul M, Sokolovski M, Kheyman M, Kakamanu S, et al. Three-dimensional sonographic findings of a cervical pregnancy. J Ultrasound Med. 2008;27(1):155–8.
134. Herbertsson G, Magnusson SS, Benediktsdottir K. Ovarian pregnancy and IUCD use in a defined complete population. Acta Obstet Gynecol Scand. 1987;66(7):607–10.
135. Ash A, Smith A, Maxwell D. Caesarean scar pregnancy. BJOG. 2007;114(3):253–63.
136. Rotas MA, Haberman S, Levgur M. Cesarean scar ectopic pregnancies: etiology, diagnosis, and management. Obstet Gynecol. 2006;107(6): 1373–81.
137. Timor-Tritsch IE, Monteagudo A. Unforeseen consequences of the increasing rate of cesarean deliveries: early placenta accreta and cesarean scar pregnancy. A review. Am J Obstet Gynecol. 2012;207(1):14–29.
138. Lipscomb GH, Bran D, McCord ML, Portera JC, Ling FW. Analysis of three hundred fifteen ectopic pregnancies treated with single-dose methotrexate. Am J Obstet Gynecol. 1998;178(6):1354–8.
139. Lipscomb GH, Stovall TG, Ling FW. Nonsurgical treatment of ectopic pregnancy. N Engl J Med. 2000;343(18):1325–9.
140. Lipscomb GH, McCord ML, Stovall TG, Huff G, Portera SG, Ling FW. Predictors of success of methotrexate treatment in women with tubal ectopic pregnancies. N Engl J Med. 1999;341(26):1974–8.
141. Tzafettas JM, Stephanatos A, Loufopoulos A, Anapliotis S, Mamopoulos M, Kalogeropoulos A. Single high dose of local methotrexate for the management of relatively advanced ectopic pregnancies. Fertil Steril. 1999;71(6):1010–3.
142. Romero R, Copel JA, Kadar N, Jeanty P, Decherney A, Hobbins JC. Value of culdocentesis in the diagnosis of ectopic pregnancy. Obstet Gynecol. 1985;65(4):519–22.
143. Vermesh M, Graczykowski JW, Sauer MV. Reevaluation of the role of culdocentesis in the management of ectopic pregnancy. Am J Obstet Gynecol. 1990;162(2):411–3.